JASN

J Am Soc Nephrol. 2014 Oct; 25(10): 2241–2253. PMCID: PMC4178447
Published online 2014 Apr 3. doi: 10.1681/ASN.2013111234

A Protein Kinase A–Independent Pathway Controlling Aquaporin 2 Trafficking as a Possible Cause for the Syndrome of Inappropriate Antidiuresis Associated with *Polycystic Kidney Disease 1* Haploinsufficiency

Grazia Tamma,[*] Domenica Lasorsa,[*] Christiane Trimpert,[†] Marianna Ranieri,[*] Annarita Di Mise,[*] Maria Grazia Mola,[*] Lisa Mastrofrancesco,[*] Olivier Devuyst,[‡] Maria Svelto,[*] Peter M.T. Deen,[†] and Giovanna Valenti[*]

[*]Department of Biosciences Biotechnologies and Biopharmaceutics, University of Bari, Bari, Italy;
[†]Department of Physiology, Radboud University Medical Centre, Nijmegen, The Netherlands; and
[‡]Institute of Physiology, University of Zurich, Zurich, Switzerland
[*]Corresponding author.
Correspondence: Dr. Grazia Tamma, Department of Bioscience, Biotechnology and Biopharmaceutics, University of Bari, Via Amendola 165/A, 70125 Bari, Italy. Email: grazia.tamma@uniba.it

Received 2013 Nov 27; Accepted 2014 Jan 22.

Abstract

Renal water reabsorption is controlled by arginine vasopressin (AVP), which binds to V2 receptors, resulting in protein kinase A (PKA) activation, phosphorylation of aquaporin 2 (AQP2) at serine 256, and translocation of AQP2 to the plasma membrane. However, AVP also causes dephosphorylation of AQP2 at S261. Recent studies showed that cyclin-dependent kinases (cdks) can phosphorylate AQP2 peptides at S261 *in vitro*. We investigated the possible role of cdks in the phosphorylation of AQP2 and identified a new PKA-independent pathway regulating AQP2 trafficking. In *ex vivo* kidney slices and MDCK-AQP2 cells, *R*-roscovitine, a specific inhibitor of cdks, increased pS256 levels and decreased pS261 levels. The changes in AQP2 phosphorylation status were paralleled by increases in cell surface expression of AQP2 and osmotic water permeability in the absence of forskolin stimulation. *R*-Roscovitine did not alter cAMP-dependent PKA activity but specifically reduced protein phosphatase 2A (PP2A) expression and activity in MDCK cells. Notably, we found reduced PP2A expression and activity and reduced pS261 levels in *Pkd1*$^{+/-}$ mice displaying a syndrome of inappropriate antidiuresis with high levels of pS256, despite unchanged AVP and cAMP. Similar to previous findings in *Pkd1*$^{+/-}$ mice, *R*-roscovitine treatment caused a significant decrease in intracellular calcium in MDCK cells. Our data indicate that reduced activity of PP2A, secondary to reduced intracellular Ca^{2+} levels, promotes AQP2 trafficking independent of the AVP–PKA axis. This pathway may be relevant for explaining pathologic states characterized by inappropriate AVP secretion and positive water balance.

In most mammals, regulation of water balance is critically dependent on water intake and excretion, which

is under control of the antidiuretic hormone arginine vasopressin (AVP). In the kidney, AVP binds to the V2 vasopressin (V2R) receptor, activating the cAMP/protein kinase A (PKA) signal transduction cascade, promoting the fusion of intracellular vesicles containing aquaporin 2 (AQP2) to the apical plasma membrane, and increasing luminal permeability.[1–3] This translocation is accompanied by AVP-dependent phosphorylation of AQP2 at serine-256 (pS256).

Mice in which S256 could not be phosphorylated (AQP2-S256L) develop polyuria and hydronephrosis because of a defect in AQP2 trafficking to the plasma membrane.[4] Interestingly, it connects to polycystic kidney disease (PKD). Mutations in polycystin-1 ($Pkd1^{+/-}$) gene cause PKD, whereas PKD1 haplo-insufficient mice ($Pkd1^{+/-}$), showing an inappropriate antidiuresis, display significantly higher levels of pS256 compared with wild-type (WT) littermates; the prominent expression at the apical plasma membrane of collecting duct principal cells, despite normal V2R expression and normal cAMP levels, is associated with unchanged AVP expression in the brain, despite chronic hypo-osmolality.[5]

These observations underscore the crucial role of AQP2 phosphorylation at S256 in controlling the cellular distribution and fate of AQP2.[1,6,7] As for many proteins, the function and the trafficking of AQP2 are modulated by a balance of reversible phosphorylation and dephosphorylation. Preventing dephosphorylation of AQP2 with okadaic acid, inhibitor of phosphatase 1 (PP1), inhibitor of phosphatase 2A (PP2A), and inhibitor of phosphatase 2B (PP2B) significantly increased AQP2-pS256.[8] Proteomic analysis of inner medulla collecting duct identified PP2A as a phosphoprotein isolated from inner medullary collecting duct samples treated with either calyculin-A, a specific PP2A inhibitor, or vasopressin,[9] suggesting the possible participation of this phosphatase in cellular events triggered by physiologic stimulus, such as vasopressin in renal collecting duct cells.

The complexity of AQP2 regulation was further increased by phosphoproteomics studies showing that, other than S256, vasopressin modulates the phosphorylation status of three other sites within the C terminus (S261, S264, and S269). Although vasopressin increases S264 and S269 phosphorylation, it decreases S261 phosphorylation.[9–12] Regarding the potential kinases responsible for the phosphorylation of these sites, c-Jun N-terminal kinase, p38, and cyclin-dependent kinases (cdks) cdk1 and cdk5 can phosphorylate AQP2 peptides at S261 *in vitro*.[13,14] Here, in the attempt to investigate the potential involvement of cdks in AQP2 regulation, we discovered a new PKA-independent signal transduction pathway regulating AQP2 phosphorylation and localization. We found that selective inhibition of cdks with *R*-roscovitine is associated with a decrease of intracellular Ca^{2+} levels and a significant downregulation of the phosphatase PP2A activity, resulting in an increase of AQP2 phosphorylation at S256 and targeting to the apical membrane. Physiologically, this novel regulatory mechanism might be of clinical interest, because it better elucidates the molecular bases of pathologic states characterized by disturbances in water balance.

Results

Renal Expression of cdks

Recent data have shown that cdk1 and cdk5 can phosphorylate AQP2 peptides at S261 *in vitro*.[14] To investigate the possible involvement of cdk1 and cdk5 in AQP2 trafficking, expression of these kinases in renal collecting ducts was evaluated. Immunoblotting analysis of mouse renal cortex and inner medulla

and outer medulla revealed specific bands of the anticipated mass of 35 kD, indicating that cdk1 and cdk5 are expressed in these tissues (Figure 1, A, upper panel, and B, upper panel). The expression of both kinases was further detected in M1, Madin–Darby canine kidney (MDCK), and mpkCCD cells, three different cell models commonly used to study the intracellular trafficking of AQP2. Immunohistochemistry further revealed that cdk1 and cdk5 localized with AQP2 in renal principal cells (Figure 1, A, lower panel, and B, lower panel). However, colocalization with AQP2 at the apical side was only seen for cdk1 (Figure 1A, upper panel).

Ex Vivo Assessment of AQP2 Trafficking under cdks Inhibition

To study the possible role of cdks on AQP2 phosphorylation and trafficking, we took advantage of *R*-roscovitine, a selective inhibitor of these kinases.[15] *Ex vivo* experiments were performed in fresh rat kidney slices incubated with or without desmopressin (dDAVP) and/or roscovitine. Subsequent immunoblotting revealed that incubation with *R*-roscovitine (R; R=3.23±0.37 versus control [CTR]=1.00±0.34, n=3, P<0.05) or dDAVP (dDAVP=2.55±0.47 versus CTR=1.00±0.34, n=3, P<0.05) significantly increased the level of pS256 compared with renal tissue left untreated (CTR) (Figure 2A). This stimulation was even further increased on cotreatment with dDAVP and *R*-roscovitine (R+dDAVP=5.50±0.31 versus CTR=1.00±0.34, n=3, P<0.05) (Figure 2A). In line with this dDAVP-like stimulation of S256 phosphorylation, *R*-roscovitine (R=0.41±0.13 versus CTR=1.00±0.14, n=3, P<0.05) and dDAVP (dDAVP=0.55±0.1 versus CTR=1.00±0.14, n=3, P<0.05) significantly reduced pS261 compared with untreated renal tissue, which was significantly further reduced on cotreatment with dDAVP and *R*-roscovitine (R+dDAVP=0.31±0.076 versus CTR=1.00±0.14, n=3, P<0.05) (Figure 2A). These further increases in pS256 and reduction in pS261 with the cotreatment compared with dDAVP and roscovitine only suggest that the effects of dDAVP and roscovitine on AQP2 are synergistic and acting through different mechanisms.

Importantly, confocal studies on renal sections revealed that, compared with untreated sections, in which AQP2 staining localized to intracellular vesicles, *R*-roscovitine and dDAVP induced AQP2 translocation to the apical membrane (Figure 2B).

In Vitro Assessment of AQP2 Trafficking under cdks Inhibition

To dissect the signal transduction pathway activated by *R*-roscovitine treatment, polarized MDCK-hAQP2 cells were used, which have been shown to be a reliable system to study intracellular trafficking regulation of AQP2 and show dDAVP/forskolin-induced changes in S256 and S261 phosphorylation *in vivo*.[11,16–18] In line with our *ex vivo* data, *R*-roscovitine, forskolin, and the combination of roscovitine and forskolin (F) significantly increased pS256 (F=2.6±0.5; R=2.00±0.22; RF=1.80±0.11 versus CTR=1.00±0.12, n=4, P<0.05) and reduced pS261 (F=0.53±0.07; R=0.41±0.06; RF=0.25±0.06 versus CTR=1.00±0.04, n=4, P<0.05) (Figure 3). The decrease in pS261 was significantly deeper on cotreatment with forskolin and *R*-roscovitine. Neither *R*-roscovitine nor dDAVP altered the intracellular level of the housekeeping protein actin (Figure 3).

As observed in renal section, confocal studies revealed that, similar to forskolin stimulation, incubation with *R*-roscovitine increased the cell surface expression of AQP2 compared with controls, a condition in which AQP2 localized in intracellular vesicles. The apical staining of AQP2 was also detected on stimulation with *R*-roscovitine and forskolin (Figure 4A). To verify whether the apical localization of

AQP2 observed by confocal studies involved its insertion into the apical plasma membrane, cell surface biotinylation experiments were performed. In line with immunocytochemistry data, *R*-roscovitine, forskolin, and their combination increased the cell surface abundance of AQP2 at the apical plasma membrane (R=1.85±0.24; F=3.53±0.69; RF=2.91±0.67 versus CTR=1.00±0.067, n=3, P<0.05) (Figure 4B, densitometry on the right). Consistent with these observations, *R*-roscovitine or forskolin treatment induced a significantly higher temporal osmotic response (reported as $1/\tau$) compared with untreated cells (1.35±0.14; 1.529±0.10 versus CTR=1.00±0.07) (Figure 4C). Altogether, these *ex vivo* and *in vitro* data indicated that inhibition of cdks increases principal cell permeability by inducing AQP2 trafficking from vesicles to the apical membrane.

Intracellular Signals Regulating AQP2 Trafficking under cdks Inhibition

Apical targeting of AQP2 depends on intracellular cAMP, which activates PKA.[1,2] To test whether *R*-roscovitine affects AQP2 trafficking by fine-tuning PKA activity, fluorescence resonance energy transfer (FRET) experiments were performed. For FRET, MDCK-hAQP2 cells were cotransfected with RII-ECFP and Cat-EYFP, and FRET signals were measured under treatments described above (Figure 5). Compared with untreated cells, normalized FRET signals decreased only with forskolin (F=70.09%±9.35%, n=72 cells; RF=64.58%±9.3% n=75 cells versus CTR=100%±7.09%, n=98 cells; R=99.89%±9.93%, n=87 cells). Consistent with FRET observations, *R*-roscovitine treatment did not lead to increased intracellular levels of cAMP (R=88.05%±10.5%; CTR=100%±19.68%), indicating that AQP2 phosphorylation and trafficking, in response to *R*-roscovitine, are independent on cAMP-dependent PKA activity.

Because *R*-roscovitine treatment results in a cAMP/PKA-independent increase in AQP2-pS256 and plasma membrane abundance of AQP2, we subsequently investigated the possible involvement of protein phosphatases in the roscovitine response. Previous studies have shown that serine/threonine phosphatases are of potential relevance to vasopressin signaling in inner medulla collecting ducts.[8,9] Immunoblotting studies revealed that *R*-roscovitine significantly decreased the PP2A abundance (R=26.54%±4,62% versus CTR=100%±22.35%, n=3, P<0.05) but not the abundance of PP1 or PP2B (Figure 6A). Consistently, analysis of the activities of PP1, PP2A, and PP2B using phosphatase-specific immunoprecitation assays[19] revealed that *R*-roscovitine treatment significantly reduced the activity of PP2A (R=61.34%±4.20% versus CTR=100%±6.829%, n=3, P<0.05) but not the activity of PP1 or PP2B (Figure 6B). No significant free phosphate was detected when unspecific IgG were used in the assay (IgG=43±6.50 versus CTR=1585±42.15 in picomoles per 25 μl). These data suggest that the increase in AQP2-pS256 and plasma membrane abundance of AQP2 with roscovitine was caused by reduced activity of PP2A.

To clarify the possible involvement of PP2A on AQP2 phosphorylation, MDCK-hAQP2 cells were incubated with calyculin-A at 50 pM to inhibit PP2A specifically, because IC_{50} values for inhibitory activity against PP1 are approximately 2 nM.[20,21] Incubation with calyculin-A increased pS256 (calyculin-A=2.00±0.58; R=2.00±0.22 versus CTR=1.00±0.12, n=4, P<0.05) and decreased pS261 (calyculin-A=0.36±0.13; R=0.33±0.06 versus CTR=1.00±0.025, n=4, P<0.05) similar to that observed with *R*-roscovitine (Figure 7). Because PP2A contained two functional and highly conserved Ca^{2+}-binding EF-hand motifs[22] modulating its activity,[23] the intracellular free calcium concentration was measured. Incubation with *R*-roscovitine significantly reduced the concentration of free calcium compared with unstimulated cells (R=193.7±7.12 nM, n=178 cells versus CTR=66.76±2.06 nM, n=236 cells, P<0.001) (

Figure 8), which might account for the decreased activity of the calcium-regulated PP2A.

Intracellular Signals Modulating Water Handling in a Model of Syndrome Of Inappropriate Antidiuretic Hormone Secretion

In a mouse model of inappropriate antidiuresis carrying a targeted deletion of *Pkd1*$^{+/-}$,[24] the aquaretic response to water load and specific V2R antagonist was reduced compared with WT mice, which coincided with unchanged levels of cAMP, AQP2, and V2R.[5] *Pkd1*$^{-/-}$ mice showed increased AQP2-pS256 and plasma membrane expression of AQP2 together with significantly decreased intracellular calcium concentrations.[5] Compared with WT, kidneys isolated from *Pkd1*$^{+/-}$ mice showed an increase in S256 phosphorylation (*Pkd1*$^{+/-}$=2.05±0.40 versus *Pkd1*$^{+/+}$=1.00±0.21, n=6, P<0.05), which has already been shown,[5] and a decrease in pS261 (*Pkd1*$^{+/-}$=0.52±0.09 versus CTR=1.00±0.18, n=6, P<0.05) (Figure 9). Considering the similarity with our proposed pathway regulating AQP2, we set out to determine whether a reduced PP2A activity could underlie the increased water retention in our *Pkd1*$^{+/-}$ mice. Interestingly, the abundance of the calcium-regulated PP2A was found significantly reduced compared with *Pkd1*$^{+/+}$ kidneys (Figure 10A) (*Pkd1*$^{+/-}$=24.81±7.31 versus *Pkd1*$^{+/+}$=100±7.34, n=6, P<0.05). Consistently, the reduced expression level was, indeed, paralleled by a decreased activity of PP2A in *Pkd1*$^{+/-}$ compared with WT counterpart (Figure 10B) (*Pkd1*$^{+/-}$=66.12±11.32 versus *Pkd1*$^{+/+}$=100±5.725, n=3, P<0.05). In contrast, no significant change in protein expression levels as well as PP1 and PP2B activities was detected in *Pkd1*$^{+/-}$ kidneys respect to WT kidneys (Figure 10B).

PP2A is known to modulate the activity of more than 30 kinases[25,26] including glycogen synthase kinase 3α (GSK3α), which is inactivated by selective phosphorylation at S21.[27] Because ongoing studies reveal the crucial role played by GSK3 in the regulation of vasopressin action in the renal collecting ducts,[28] the phosphorylation status of GSK3α was investigated here. In line with a reduced expression and activity of PP2A, the phosphorylation level of GSK3α was significantly higher in *Pkd1*$^{+/-}$ mice compare with WT animals (*Pkd1*$^{+/-}$=2.90±0.74 versus *Pkd1*$^{+/+}$=100±0.05, P<0.05) (Figure 11A). Interestingly, pGSK3α was found significantly increased under roscovitine treatment or selective inhibition of PP2A with calyculin-A in fresh kidney slices (R=2.23±0.19; calyculin-A=3.49±0.67, n=4, P<0.05), likely strengthening the similarity of *Pkd1*$^{+/-}$ animal model and our novel proposed pathway regulating AQP2.

Discussion

The major finding of this study is the identification of a new PKA-independent pathway regulating AQP2 trafficking. Specifically, our data indicate that reduced activity of PP2A, secondary to reduced intracellular Ca^{2+} levels, promotes AQP2 trafficking independently of the AVP–PKA axis. The experimental strategy leading to these results has been the pharmacological inhibition of cdks with *R*-roscovitine. We found that *R*-roscovitine mimics the cellular response exerted by AVP stimulation, because it affects the phosphorylation and increases the cell surface–expressed AQP2. Surprisingly, *R*-roscovitine–induced AQP2 relocalization at the apical plasma membrane occurs independently of cAMP-dependent PKA stimulation, indicating that *R*-roscovitine does not alter cAMP concentration at steady state and suggesting the existence of an alternative PKA-independent pathway controlling AQP2 trafficking.

Involvement of Protein Phosphatases in the Regulation of AQP2 Phosphorylation

Focusing our studies on protein phosphatases, which are potentially relevant to vasopressin response, we show here that *R*-roscovitine specifically reduces the activity of PP2A. The reduced expression and activity of PP2A found in cells pretreated with *R*-roscovitine is consistent with the observed increase in AQP2-pS256. The specific association between reduction of PP2A expression and increase in AQP2-pS256 was shown by treatment of intact cells with calyculin-A, resulting in an increase in pS256-AQP2. Calyculin-A is a strong phosphatase inhibitor displaying effect on PP2A (IC_{50} approximately 0.5–1 nM) and less effect on PP1 (IC_{50} approximately 2 nM), two phosphatases sharing some degree of redundancy.[29,30] To reach a specific effect to PP2A, MDCK cells were treated with 50 pM calyculin-A.

The highest phosphorylation level of pS256, on cotreatment with *R*-roscovitine and dDAVP, underscores the selective activation of alternative signaling pathways by *R*-roscovitine and dDAVP, respectively. Because PP2A contains two functional and highly conserved Ca^{2+}-binding EF-hand motifs,[22] it can be speculated that the observed decrease in intracellular calcium concentration, associated with *R*-roscovitine treatment, might be responsible for the strong reduction in PP2A activity observed *in vivo* and in intact cells.

In this context, it seems that intracellular calcium decrease is a pivotal upstream condition leading to PP2A downregulation. Although our recent data provide an explanation for this effect in renal cells, showing that *R*-roscovitine causes a significant increase in calcium content in the endoplasmic reticulum because of an increase in sarco/endoplasmic reticulum Ca^{2+}-ATPase activity,[31] it is not known why low intracellular calcium is observed in inner medulla of *Pkd1*$^{+/-}$ mice.

Other than affecting PP activities, reduced cytosolic calcium might also regulate the local activity of the calcium-dependent adenylyl cyclases and/or phosphodiesterases, which in turn, might modulate cAMP level in specific intracellular microdomains.

PP2A Inhibition Can Explain the Syndrome Of Inappropriate Antidiuresis Phenotype Observed in *Pkd1*$^{+/-}$ Mice

Pkd1$^{+/-}$ mice had a decreased aquaretic response to both a water load and a selective V2R antagonist. Moreover, in those mice, cAMP levels in kidney and urine were unchanged along with the mRNA levels of AQP2. Nevertheless, AQP2-pS256 levels were upregulated,[5] whereas pS261 decreased, with a prominent distribution on the apical membrane of collecting duct principal cells. Of note, these mice have significantly lower intracellular basal calcium content in renal collecting ducts compared with WT mice.[5] These features correspond to the similar effects described here in *R*-roscovitine–treated MDCK cells.

In addition, analysis of different phosphatases expression and activities revealed a significant decrease in the protein expression of the calcium-regulated PP2A, which was paralleled by a significant reduction of its activity. This result might explain the observed increase in S256 phosphorylation.[5] However, the reduced expression and activity of PP2A in *Pkd1*$^{+/-}$ mice and MDCK cells on *R*-roscovitine incubation do not explain directly the observed decreased pS261, which instead, might be a consequence of the increased pS256 (as a priming phosphorylation event). Alternatively, it can be speculated that PP2A downregulation results in a selective inhibition of GSK3α, a known PP2A target substrate[25] that is negatively regulated by phosphorylation at S21. As shown here, in *Pkd1*$^{+/-}$ mice and renal kidney slices, GSK3α phosphorylation at S21 significantly increased under roscovitine treatment. Of note, using the NetPhosk 1.0 server, S261 is

designed as a potential phosphorylation site for GSK3.

We could not evaluate modulation of GSK3α phosphorylation in MDCK cells, because no specific immunoreactive band was detected in MDCK cells with the available anti-GSK3α and anti–GSK3α-pS21 antibodies. Involvement of GSK3β could be excluded, because no change in its phosphorylation level was detected in MDCK cells under roscovitine treatment (data not shown). In addition, GSK3β phosphorylation and activity are under control of PP1,[26] which was found unchanged at protein level and activity, whereas PP2A is selective for pGSK3α and not pGSK3β[27]. These observations led us to speculate that PP2A inhibition might reduce S261 phosphorylation through inhibition of GSK3α, because its phosphorylation level was found increased in *Pkd1*$^{+/-}$ mice and fresh renal tissue under roscovitine and calyculin-A.

Furthermore, we have to point out that, in *Pkd1*$^{+/-}$ mice, the calcium-regulated PP2B was unaffected in terms of both expression and activity, similar to that observed in MDCK cells. This finding suggests that this protein phosphatase does not play a direct role in controlling AQP2 phosphorylation and trafficking in this animal model.

Considering the similarity of *Pkd1*$^{+/-}$ animal model and *R*-roscovitine action in MDCK cells, we propose a new PKA-independent signal transduction pathway promoting AQP2 trafficking. Specifically, our studies reveal that (*1*) *R*-roscovitine reduces the phosphorylation level of AQP2 at S261 through cdk1 and cdk5; (*2*) *R*-roscovitine decreases intracellular calcium level, reducing the activity of PP2A; and (*3*) the decrease of PP2A activity is paralleled by a significant increase in pS256 and a decrease in pS261 through GSK3α inhibition, facilitating AQP2 targeting to the plasma membrane (Figure 12). To conclude, by identifying PP2A as a selective phosphatase downregulated in either *R*-roscovitine–treated cells and *Pkd1*$^{+/-}$ mice, we provide here new insights into the mechanisms that govern the syndrome of inappropriate antidiuresis phenotype characterized by positive water balance associated with upregulation of S256 AQP2.

Concise Methods

Chemicals and Reagents

To detect the total amount of AQP2, we used antibodies against the 20-amino acid residue segment just N-terminal from the polyphosphorylated region of rat AQP2 (CLKGLEPDTDWEEREVRRRQ).[9,32] AQP2-pS256 antibodies were as described in the work by Trimpert *et al*.[33] AQP2-pS261 antibodies were purchased from Novus Biologic. Antibodies specific for cdk1, cdk5, PP1, PP2B, GSK3α, and GSK3α-pS21 were purchased from Santa Cruz Biotechnology. *R*-roscovitine, dDAVP, calyculin-A, and protein A-Sepharose were purchased from Sigma-Aldrich. Calcein-AM was obtained from Life Techonologies. Biocytin Hydrazide and streptavidin beads were purchased from EZ-Link Pierce. The PP2A Immunoprecipitation Phosphatase Assay Kit and the PP2A antibodies were purchased from EMD Millipore.

Cell Culture and Treatments

MDCK-hAQP2 type I cells, stably expressing human AQP2, were grown as described.[34] In brief, they were grown in DMEM supplemented with 5% (v/v) FCS at 37°C in 5% CO_2. MDCK cells were seeded at

1.5×10^5 cells/cm^2 and grown to confluence for 4 days. After overnight treatment with indomethacin (5×10^{-5} M), cells were left under basal condition or stimulated with forskolin (10^{-5} M for 45 minutes) or calyculin-A (50 pM for 1 hour). Alternatively, cells were incubated overnight with *R*-roscovitine (10 μM), a selective inhibitor of cdks and then, left unstimulated or stimulated with forskolin (10^{-5} M for 45 minutes). As reported,[34] addition of the prostaglandin synthesis inhibitor indomethacin was needed to reduce basal cAMP and AQP2-pS256 levels[12,34] and was present in all treatments.

Ex Vivo Preparation

Ex vivo studies were performed as reported.[35] Briefly, male Sprague–Dawley rats were anesthetized and euthanized by decapitation. Kidneys were quickly removed, and sections of approximately 0.5 mm were made and divided in four groups. The sections were equilibrated for 10 minutes in a buffer containing 118 mM NaCl, 16 mM Hepes, 17 mM Na-Hepes, 14 mM glucose, 3.2 mM KCl, 2.5 mM $CaCl_2$, 1.8 mM $MgSO_4$, and 1.8 mM KH_2PO_4 (pH 7.4). AQP2 trafficking was stimulated in the same buffer at 37°C with 1 nM dDAVP for 45 minutes with either 10 μM *R*-roscovitine in the absence or presence of dDAVP or calyculin-A for 1 hour. The treated sections were subjected to immunofluorescence or immunoprecipitation studies. The animal experiments performed were approved by the Ministry of Health (authorization no. 23/98-A), and animals were housed according to local and international requirements.

Immunofluorescence

Immunocytochemistry was performed as described.[36] Briefly, MDCK-hAQP2 cells were grown, treated as described above, and fixed for 30 minutes with 4% paraformaldehyde in PBS. Alternatively, kidney slices were fixed overnight in 4% paraformaldehyde at 4°C, infiltrated with 30% sucrose in PBS for 24 hours, embedded in Cryomatrix (DDK Srl) in dry ice, and cut with a cryostat to obtain 5-μm sections. After quenching of aldehyde groups with 50 mM NH_4Cl in PBS for 15 minutes, samples were permeabilized with 0.1% Triton X-100 in PBS for 5 minutes, blocked with 1% PBS-BSA for 30 minutes, and incubated overnight with a 1:1000 dilution of AQP2 antibodies. Kidney sections were costained with cdk1 (1:100) or cdk5 (1:100) antibodies. After washing three times with PBS-BSA, samples were incubated with 1:1000 diluted goat anti-rabbit antibodies coupled to Alexa-488 or donkey anti-mouse antibodies coupled to Alexa-555 (Molecular Probes) in PBS-BSA for 1 hour. Next, cells or kidney sections were rinsed three times with PBS and mounted on glass slides with Mowiol. Images were obtained with a Leica TCS SP2 camera (Leica Microsystems).

Immunoprecipitation

Immunoprecipitation experiments were performed as described.[32,37] Briefly, cells or rat kidney slices were treated as described above and lysed with 1% Triton X-100, 150 mM NaCl, and 25 mM Hepes (pH 7.4) in presence of proteases inhibitors (1 mM PMSF, 2 mg/ml leupeptin, and 2 mg/ml pepstatin A). Supernatants were precleared with 50 μl immobilized protein-A and incubated overnight with anti-AQP2 antibodies coupled to protein A Sepharose. Immunocomplexes were washed three times, resuspended in 50 μl Laemmli's buffer, and subjected to immunoblotting using AQP2, AQP2-pS256, and AQP2-pS261 antibodies. Alternatively, total lysates were immunoblotted with GSK3α and GSK3α-pS21 antibodies.

Cell Surface Biotinylation

Biotinylation was carried out according to the protocols provided by the manufacturer (Pierce) with some adaptations as described.[32] MDCK-hAQP2 cells were cultured on six-well filters in DMEM for 4 days and treated as described above. Cells were washed thoroughly with ice-cold Coupling Buffer (0.1 M sodium phosphate and 0.15 M NaCl [pH 7.2]) before being subjected to oxidation with Na^+ metaperiodate (20 mM) in Coupling Buffer for 30 minutes on ice in the dark. After three rounds of washing with Coupling Buffer, cell surface glycoproteins were labeled with 5 mM Biocytin Hydrazide (EZ-Link Pierce) for 30 minutes. The biotinylation buffer was removed; cells were incubated with quenching solution (50 mM NH_4Cl in PBS at pH 7.2) for 5 minutes and washed three times with Coupling Buffer. Cells were solubilized with lysis buffer (1% Triton X-100 and 0.01% SDS in PBS) supplemented with 2 μg/ml pepstatin-A, 2 μg/ml leupeptin, and 2 mM PMSF for 30 minutes. The lysates were homogenized using an ultrasonic homogenizer at 40 Hz for 20 seconds and centrifuged at 12,000×*g* for 20 minutes. An aliquot of the supernatants (20 μl) was diluted in Laemmli's buffer, whereas the remaining biotinylated proteins were pulled down with immobilized streptavidin beads. The complexes were washed three times with Wash Buffer (Triton X-100 0.5% and SDS 0.01% in PBS), denatured in Laemmli's buffer for 30 minutes at 37°C, and analyzed by SDS-PAGE and immunoblotting.

Immunoblotting

SDS-PAGE, blotting, blocking, antibody incubation, and chemiluminescence of the membranes have been described.[38] AQP2, AQP2-pS256, and AQP2-pS261 were used at 1:1000 dilutions; cdk1, cdk5, PP1, and PP2A antibodies were used at 1:500, whereas PP2B was diluted 1:300. GSK3α and GSK3α-pS21 were used at 1:200 dilutions. Secondary antibodies goat anti-rabbit or goat anti-mouse horseradish peroxidase–coupled antibodies were used. Representative figures are shown. Densitometry analysis was performed using Scion image. Data (in arbitrary units) are summarize in histograms by using GraphPad Prism.

Statistical Analyses

One-way ANOVA followed by a Newman–Keuls multiple comparison test was used for the statistical analysis. When applicable, *t* test was also used. All values are expressed as means±SEM. A difference of $P<0.05$ was considered statistically significant.

Water Permeability Assay

Osmotic water permeability was measured as shown by Mola *et al*.[39] A benchtop fluorescence plate reader (FlexStation II; Molecular Devices, MDS Analytical Technologies) equipped to analyze real-time fluorescence kinetic data in a 96-well format was used. Data acquisition was performed by Soft Max Pro software, and the data were analyzed with Prism (GraphPad Software Inc.) software. MDCK-hAQP2 cells were seeded in 96-well black-walled microplates (Corning Costar Corp.), and water permeability assays were done at 24–48 hours after plating, at which time cells were 90% confluent. Cells were washed with PBS and incubated at 37°C for 45 minutes with 10 μM membrane permeable Calcein-AM. Fluorescence was excited at 490 nm and detected at 520 nm using dual monochromators. Time course fluorescence data after mixing of cells with hypo- or isosmotic solutions were recorded over an 80-second period. The time constant of cell swelling because of the hypotonic stimulus was obtained by fitting data with an exponential function.[39]

Transient Expression

MDCK cells were seeded 1 day before transfection at 80% confluence; 25 μl polyethylenimine (1 μg/μl) was dissolved with 25 μl 150 mM NaCl and incubated for 5 minutes at room temperature. In parallel, 1 μg DNA was diluted in 150 mM NaCl to a final volume of 50 μl. After 5 minutes, solutions were mixed and incubated for 20 minutes at room temperature. Transfecting solution was then added to 2 ml complete medium and incubated for 8 hours. FRET experiments were executed 48 hours after transfection.

Video Imaging Measurements

In the fluorescence measurements, the coverslips with dye-loaded cells were mounted in a perfusion chamber (FCS2 Closed Chamber System; BIOPTECHS), and measurements were performed using an inverted microscope (Nikon Eclipse TE2000-S microscope) equipped for single cell fluorescence measurements and imaging analysis. The sample was illuminated through a 40× oil immersion objective (numerical aperture=1.30).

FRET Measurements

FRET experiments were performed as described.[32,40] Briefly, MDCK cells were transiently cotransfected with plasmids encoding the regulatory and catalytic subunits of PKA fused to cyan fluorescent protein (ECFP) and yellow fluorescent protein (EYFP), respectively (1 μg per each plasmid), using the polyethylenimine procedure already described.[32] RII-ECFP and C-EYFP have been described[41] and were provided by M. Zaccolo. Specifically, in the condition of low cAMP, the fluorescent probes-tagged PKA subunits are in inactive holotetrameric conformation, and FRET is maximal. When cAMP rises, the second messenger binds to RII-CFP, resulting in a conformational change that releases active C-EYFP; CFP and YFP diffuse apart, and FRET is significantly reduced. ECFP and EYFP were excited at 430 and 480 nm, respectively; fluorescence emitted from ECFP and EYFP was measured at 480/30 and 545/35 nm, respectively. FRET from ECFP to EYFP was determined by excitation of ECFP and measurement of fluorescence emitted from EYFP. Corrected normalized FRET values were determined according to the work by Ritter *et al*.[40]

cAMP Measurement

MDCK cells were seeded on filters for 3 days and incubated for the last 16 hours with *R*-roscovitine or left untreated. To accumulate cAMP, cells were treated with 0.1 mM phosphodiesterase inhibitor 3-isobutyl-1-methylxanthine (Sigma-Aldrich). cAMP was measured using the cAMP enzyme immunoassay kit (Sigma-Aldrich) according to the manufacturer's instructions. Results were related to a standard curve based on the measurement of defined cAMP solutions.

Intracellular Calcium Calibration

MDCK cells were loaded with 4 μM Fura 2-AM for 15 minutes at 37°C in DMEM. Ringer's solution was used to perfuse cells during the experiment containing 140 mM NaCl, 5 mM KCl, 1 mM $MgCl_2$, 10 mM Hepes, 5 mM glucose, and 1 mM $CaCl_2$ (pH 7.4). The Fura 2-AM loaded sample was excited at 340 and 380 nm. Emitted fluorescence was passed through a dichroic mirror, filtered at 510 nm (Omega Optical), and captured by a cooled CCD camera (CoolSNAP HQ; Photometrics). Fluorescence measurements were carried out using Metafluor software (Molecular Devices, MDS Analytical Technologies).

To calibrate Fura 2, cells were treated with 5 μM ionomycin and 1 mM EGTA in Ca^{2+} free to obtain R_{min}

followed by 5 μM ionomycin and 5 mM Ca^{2+} in Ringer's solution to obtain R_{max}.

The standard equation, $[Ca^{2+}]_I$=Kd (R−R_{min})/(R_{max}−R)×Sf/Sb, was used to convert the Fura 2 340/380 ratio to $[Ca^{2+}]_{cytosol}$, where Sf and Sb are the emission intensities at 380 nm for Ca^{2+}-free and Ca^{2+}-bound Fura 2, respectively, and K_d is calculated for Fura 2 equally to 224 nmol/L. R_{min} and R_{max} are the ratio values at minimum and maximum stimuli, respectively.[42] Data are reported as mean±SEMs, with *n* equal to the number of cells. The significance of the observations was evaluated by *t* test for paired data, with $P<0.05$ considered to be statistically different.

PP Activities Assay

The protocol used a PP2A activity assay kit with some adaptations as described.[19] Cells were treated as mentioned above and lysed according to the protocol provided by the reagent manufacturer (EMD Millipore spa). Alternatively, kidneys isolated from *Pkd1*$^{+/+}$ or *Pkd1*$^{+/-}$ mice were lysed; 300 μg proteins from cell or kidney lysate, determined with Qubit (Invitrogen), were incubated with 25 μl protein-A agarose and 4 μl anti-PP1, anti-PP2A, or PP2B antibodies. After 2 hours of incubation, immunocomplexes were washed three times with ice-cold Tris-buffered saline and one time with Ser/Thr phosphopeptide buffer. After the last wash, 60 μl diluted phosphopeptide (750 μM) and 20 μl phosphopeptide buffer were added and incubated for 10 minutes at 30°C in a shaking incubator; 25 μl supernatant was placed in a 96-well plate, and a malachite green detection assay was used to determine free phosphates. A calibration curve was generated to establish the level of phosphatase activity, which is reported in picomoles of phosphate released per 25 μl supernatant.

Disclosures

None.

Acknowledgments

This study was funded by a grant from the University of Bari (Idea Giovani 2011), Research Program of National Interest (PRIN) Project Tamma01373409Prin (to G.T.), and Telethon Grant GGP13227 (to G.T. and G.V.). These studies were supported, in part, by an Action de Recherche Concertée (ARC; Communauté Française de Belgique), the Fonds National de la Recherche Scientifique (FNRS), the Fonds de la Recherche Scientifique Médicale (FRSM), and the Inter-University Attraction Pole (IUAP; Belgium Federal Government).

Footnotes

Published online ahead of print. Publication date available at www.jasn.org.

References

1. Tamma G, Procino G, Svelto M, Valenti G.: Cell culture models and animal models for studying the patho-physiological role of renal aquaporins. Cell Mol Life Sci 69: 1931–1946, 2012 [PubMed: 22189994]

2. Valenti G, Procino G, Tamma G, Carmosino M, Svelto M.: Minireview: Aquaporin 2 trafficking. Endocrinology 146: 5063–5070, 2005 [PubMed: 16150901]

3. Fenton RA, Pedersen CN, Moeller HB.: New insights into regulated aquaporin-2 function. Curr Opin

Nephrol Hypertens 22: 551–558, 2013 [PubMed: 23852332]

4. McDill BW, Li SZ, Kovach PA, Ding L, Chen F.: Congenital progressive hydronephrosis (cph) is caused by an S256L mutation in aquaporin-2 that affects its phosphorylation and apical membrane accumulation. Proc Natl Acad Sci U S A 103: 6952–6957, 2006 [PMCID: PMC1459000] [PubMed: 16641094]

5. Ahrabi AK, Terryn S, Valenti G, Caron N, Serradeil-Le Gal C, Raufaste D, Nielsen S, Horie S, Verbavatz JM, Devuyst O.: PKD1 haploinsufficiency causes a syndrome of inappropriate antidiuresis in mice. J Am Soc Nephrol 18: 1740–1753, 2007 [PubMed: 17475819]

6. Moeller HB, Olesen ET, Fenton RA.: Regulation of the water channel aquaporin-2 by posttranslational modification. Am J Physiol Renal Physiol 300: F1062–F1073, 2011 [PubMed: 21307124]

7. Brown D, Hasler U, Nunes P, Bouley R, Lu HA.: Phosphorylation events and the modulation of aquaporin 2 cell surface expression. Curr Opin Nephrol Hypertens 17: 491–498, 2008 [PMCID: PMC3774073] [PubMed: 18695390]

8. Valenti G, Procino G, Carmosino M, Frigeri A, Mannucci R, Nicoletti I, Svelto M.: The phosphatase inhibitor okadaic acid induces AQP2 translocation independently from AQP2 phosphorylation in renal collecting duct cells. J Cell Sci 113: 1985–1992, 2000 [PubMed: 10806109]

9. Hoffert JD, Pisitkun T, Wang G, Shen RF, Knepper MA.: Quantitative phosphoproteomics of vasopressin-sensitive renal cells: Regulation of aquaporin-2 phosphorylation at two sites. Proc Natl Acad Sci U S A 103: 7159–7164, 2006 [PMCID: PMC1459033] [PubMed: 16641100]

10. Fenton RA, Moeller HB, Hoffert JD, Yu MJ, Nielsen S, Knepper MA.: Acute regulation of aquaporin-2 phosphorylation at Ser-264 by vasopressin. Proc Natl Acad Sci U S A 105: 3134–3139, 2008 [PMCID: PMC2268597] [PubMed: 18287043]

11. Hoffert JD, Nielsen J, Yu MJ, Pisitkun T, Schleicher SM, Nielsen S, Knepper MA.: Dynamics of aquaporin-2 serine-261 phosphorylation in response to short-term vasopressin treatment in collecting duct. Am J Physiol Renal Physiol 292: F691–F700, 2007 [PubMed: 16985212]

12. Tamma G, Robben JH, Trimpert C, Boone M, Deen PM.: Regulation of AQP2 localization by S256 and S261 phosphorylation and ubiquitination. Am J Physiol Cell Physiol 300: C636–C646, 2011 [PubMed: 21148409]

13. Nedvetsky PI, Tabor V, Tamma G, Beulshausen S, Skroblin P, Kirschner A, Mutig K, Boltzen M, Petrucci O, Vossenkämper A, Wiesner B, Bachmann S, Rosenthal W, Klussmann E.: Reciprocal regulation of aquaporin-2 abundance and degradation by protein kinase A and p38-MAP kinase. J Am Soc Nephrol 21: 1645–1656, 2010 [PMCID: PMC3013543] [PubMed: 20724536]

14. Rinschen MM, Yu MJ, Wang G, Boja ES, Hoffert JD, Pisitkun T, Knepper MA.: Quantitative phosphoproteomic analysis reveals vasopressin V2-receptor-dependent signaling pathways in renal collecting duct cells. Proc Natl Acad Sci U S A 107: 3882–3887, 2010 [PMCID: PMC2840509] [PubMed: 20139300]

15. Meijer L, Borgne A, Mulner O, Chong JP, Blow JJ, Inagaki N, Inagaki M, Delcros JG, Moulinoux JP.: Biochemical and cellular effects of roscovitine, a potent and selective inhibitor of the cyclin-dependent

kinases cdc2, cdk2 and cdk5. Eur J Biochem 243: 527–536, 1997 [PubMed: 9030781]

16. van Balkom BW, Savelkoul PJ, Markovich D, Hofman E, Nielsen S, van der Sluijs P, Deen PM.: The role of putative phosphorylation sites in the targeting and shuttling of the aquaporin-2 water channel. J Biol Chem 277: 41473–41479, 2002 [PubMed: 12194985]

17. Moeller HB, Praetorius J, Rützler MR, Fenton RA.: Phosphorylation of aquaporin-2 regulates its endocytosis and protein-protein interactions. Proc Natl Acad Sci U S A 107: 424–429, 2010 [PMCID: PMC2806726] [PubMed: 19966308]

18. de Mattia F, Savelkoul PJ, Kamsteeg EJ, Konings IB, van der Sluijs P, Mallmann R, Oksche A, Deen PM.: Lack of arginine vasopressin-induced phosphorylation of aquaporin-2 mutant AQP2-R254L explains dominant nephrogenic diabetes insipidus. J Am Soc Nephrol 16: 2872–2880, 2005 [PubMed: 16120822]

19. Bales JW, Yan HQ, Ma X, Li Y, Samarasinghe R, Dixon CE.: The dopamine and cAMP regulated phosphoprotein, 32 kDa (DARPP-32) signaling pathway: A novel therapeutic target in traumatic brain injury. Exp Neurol 229: 300–307, 2011 [PMCID: PMC3110667] [PubMed: 21376040]

20. Cohen P.: The structure and regulation of protein phosphatases. Annu Rev Biochem 58: 453–508, 1989 [PubMed: 2549856]

21. Ishihara H, Martin BL, Brautigan DL, Karaki H, Ozaki H, Kato Y, Fusetani N, Watabe S, Hashimoto K, Uemura D, Hartshorne DJ.: Calyculin A and okadaic acid: Inhibitors of protein phosphatase activity. Biochem Biophys Res Commun 159: 871–877, 1989 [PubMed: 2539153]

22. Janssens V, Jordens J, Stevens I, Van Hoof C, Martens E, De Smedt H, Engelborghs Y, Waelkens E, Goris J.: Identification and functional analysis of two Ca2+-binding EF-hand motifs in the B"/PR72 subunit of protein phosphatase 2A. J Biol Chem 278: 10697–10706, 2003 [PubMed: 12524438]

23. Fernandez E, Schiappa R, Girault JA, Le Novère N.: DARPP-32 is a robust integrator of dopamine and glutamate signals. PLOS Comput Biol 2: e176, 2006 [PMCID: PMC1761654] [PubMed: 17194217]

24. Muto S, Aiba A, Saito Y, Nakao K, Nakamura K, Tomita K, Kitamura T, Kurabayashi M, Nagai R, Higashihara E, Harris PC, Katsuki M, Horie S.: Pioglitazone improves the phenotype and molecular defects of a targeted Pkd1 mutant. Hum Mol Genet 11: 1731–1742, 2002 [PubMed: 12095915]

25. Millward TA, Zolnierowicz S, Hemmings BA.: Regulation of protein kinase cascades by protein phosphatase 2A. Trends Biochem Sci 24: 186–191, 1999 [PubMed: 10322434]

26. Hernández F, Langa E, Cuadros R, Avila J, Villanueva N.: Regulation of GSK3 isoforms by phosphatases PP1 and PP2A. Mol Cell Biochem 344: 211–215, 2010 [PubMed: 20652371]

27. Sutherland C, Leighton IA, Cohen P.: Inactivation of glycogen synthase kinase-3 beta by phosphorylation: New kinase connections in insulin and growth-factor signalling. Biochem J 296: 15–19, 1993 [PMCID: PMC1137648] [PubMed: 8250835]

28. Rao R.: Glycogen synthase kinase-3 regulation of urinary concentrating ability. Curr Opin Nephrol Hypertens 21: 541–546, 2012 [PMCID: PMC3759996] [PubMed: 22691876]

29. Redden JM, Dodge-Kafka KL.: AKAP phosphatase complexes in the heart. J Cardiovasc Pharmacol

58: 354–362, 2011 [PMCID: PMC3158305] [PubMed: 21562429]

30. Shi Y, Reddy B, Manley JL.: PP1/PP2A phosphatases are required for the second step of Pre-mRNA splicing and target specific snRNP proteins. Mol Cell 23: 819–829, 2006 [PubMed: 16973434]

31. Tamma G, Ranieri M, Di Mise A, Spirlì A, Russo A, Svelto M, Valenti G.: Effect of roscovitine on intracellular calcium dynamics: Differential enantioselective responses. Mol Pharm 10: 4620–4628, 2013 [PubMed: 24168213]

32. Tamma G, Lasorsa D, Ranieri M, Mastrofrancesco L, Valenti G, Svelto M.: Integrin signaling modulates AQP2 trafficking via Arg-Gly-Asp (RGD) motif. Cell Physiol Biochem 27: 739–748, 2011 [PubMed: 21691091]

33. Trimpert C, van den Berg DT, Fenton RA, Klussmann E, Deen PM.: Vasopressin increases S261 phosphorylation in AQP2-P262L, a mutant in recessive nephrogenic diabetes insipidus. Nephrol Dial Transplant 27: 4389–4397, 2012 [PubMed: 22778181]

34. Deen PM, Rijss JP, Mulders SM, Errington RJ, van Baal J, van Os CH.: Aquaporin-2 transfection of Madin-Darby canine kidney cells reconstitutes vasopressin-regulated transcellular osmotic water transport. J Am Soc Nephrol 8: 1493–1501, 1997 [PubMed: 9335376]

35. Boone M, Kortenoeven ML, Robben JH, Tamma G, Deen PM.: Counteracting vasopressin-mediated water reabsorption by ATP, dopamine, and phorbol esters: Mechanisms of action. Am J Physiol Renal Physiol 300: F761–F771, 2011 [PubMed: 21209006]

36. Tamma G, Klussmann E, Oehlke J, Krause E, Rosenthal W, Svelto M, Valenti G.: Actin remodeling requires ERM function to facilitate AQP2 apical targeting. J Cell Sci 118: 3623–3630, 2005 [PubMed: 16046477]

37. Kamsteeg EJ, Hendriks G, Boone M, Konings IB, Oorschot V, van der Sluijs P, Klumperman J, Deen PM.: Short-chain ubiquitination mediates the regulated endocytosis of the aquaporin-2 water channel. Proc Natl Acad Sci U S A 103: 18344–18349, 2006 [PMCID: PMC1838753] [PubMed: 17101973]

38. Tamma G, Klussmann E, Procino G, Svelto M, Rosenthal W, Valenti G.: cAMP-induced AQP2 translocation is associated with RhoA inhibition through RhoA phosphorylation and interaction with RhoGDI. J Cell Sci 116: 1519–1525, 2003 [PubMed: 12640036]

39. Mola MG, Nicchia GP, Svelto M, Spray DC, Frigeri A.: Automated cell-based assay for screening of aquaporin inhibitors. Anal Chem 81: 8219–8229, 2009 [PMCID: PMC2850055] [PubMed: 19705854]

40. Ritter M, Ravasio A, Jakab M, Chwatal S, Fürst J, Laich A, Gschwentner M, Signorelli S, Burtscher C, Eichmüller S, Paulmichl M.: Cell swelling stimulates cytosol to membrane transposition of ICln. J Biol Chem 278: 50163–50174, 2003 [PubMed: 12970357]

41. Zaccolo M, Pozzan T.: Discrete microdomains with high concentration of cAMP in stimulated rat neonatal cardiac myocytes. Science 295: 1711–1715, 2002 [PubMed: 11872839]

42. Grynkiewicz G, Poenie M, Tsien RY.: A new generation of Ca2+ indicators with greatly improved fluorescence properties. J Biol Chem 260: 3440–3450, 1985 [PubMed: 3838314]

Figures and Tables

Figure 1.

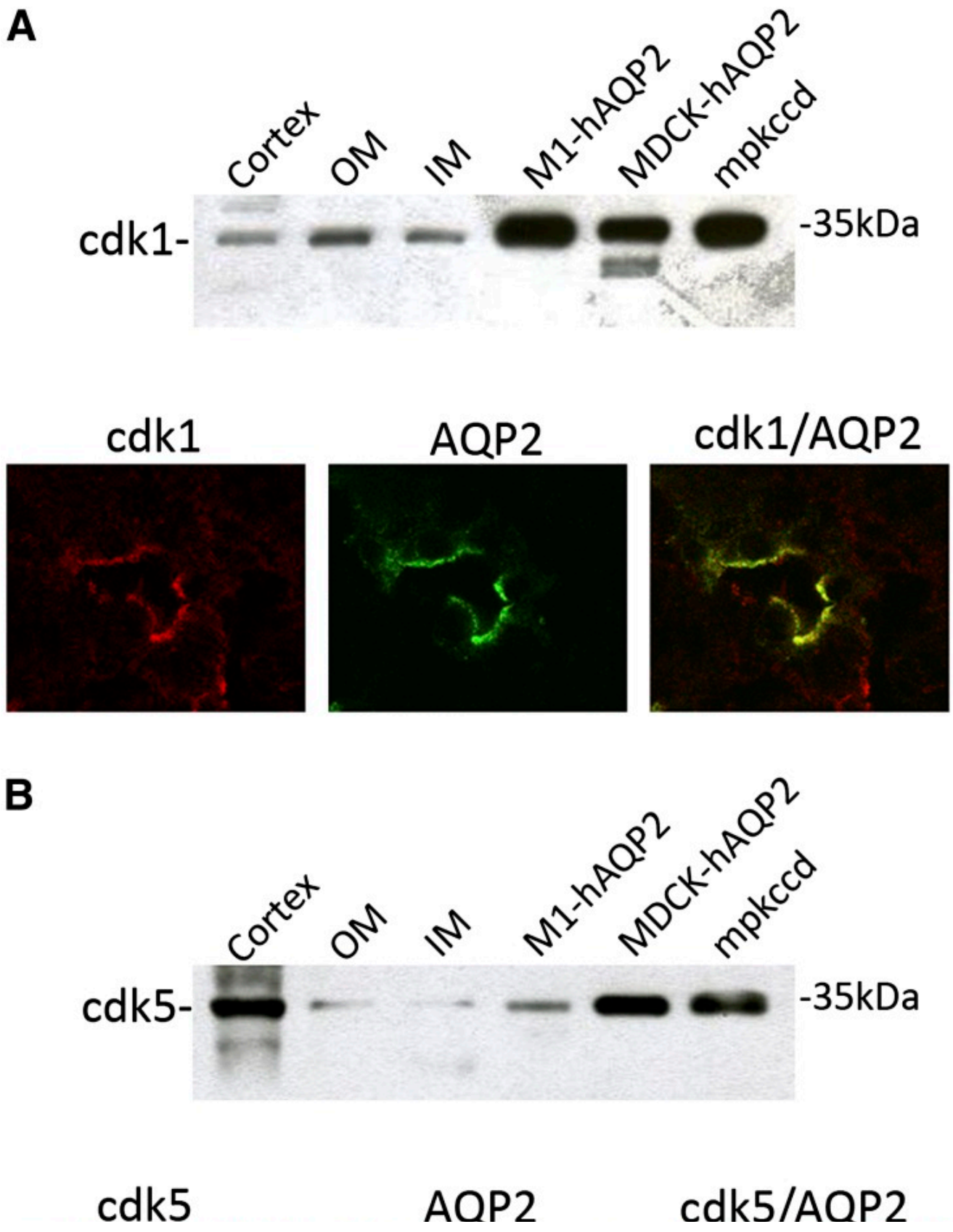

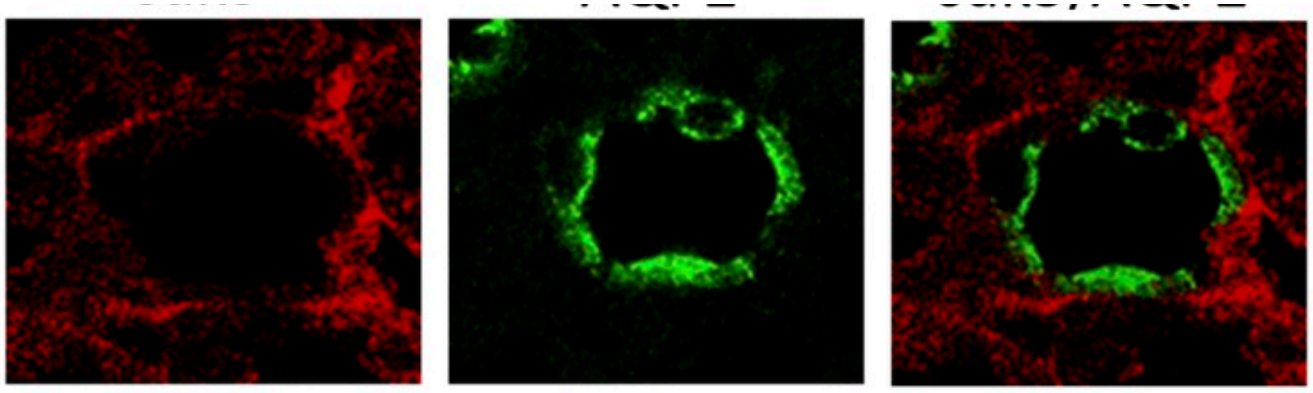

Expression and distribution of cdk1 and cdk5 in the kidney and renal cells. Immunoblot (upper panels) and immunohistochemical (lower panels) analysis of (A) cdk1 or (B) cdk5 in kidney cortex, outer medulla (OM), inner (IM) medulla, and three different cell models (M1, MDCK, and mpkCCD cells) used to study AQP2 trafficking. For immunoblotting, equal amounts of proteins from renal fractions (15 μg/lane) and cells (30 μg/lane) were immunoblotted using specific antibodies against cdk1 or cdk5. The mass of cdk1/5 is indicated on the right. Immunohistochemistry: renal sections were incubated with (A) cdk1-, (B) cdk5-, and AQP2-specific antibodies, and collecting ducts expression was analyzed using confocal imaging. Cdk1 and AQP2 colocalized in renal principal cells. Cdk5 and AQP2 were expressed in principal cells but did not colocalize.

Figure 2.

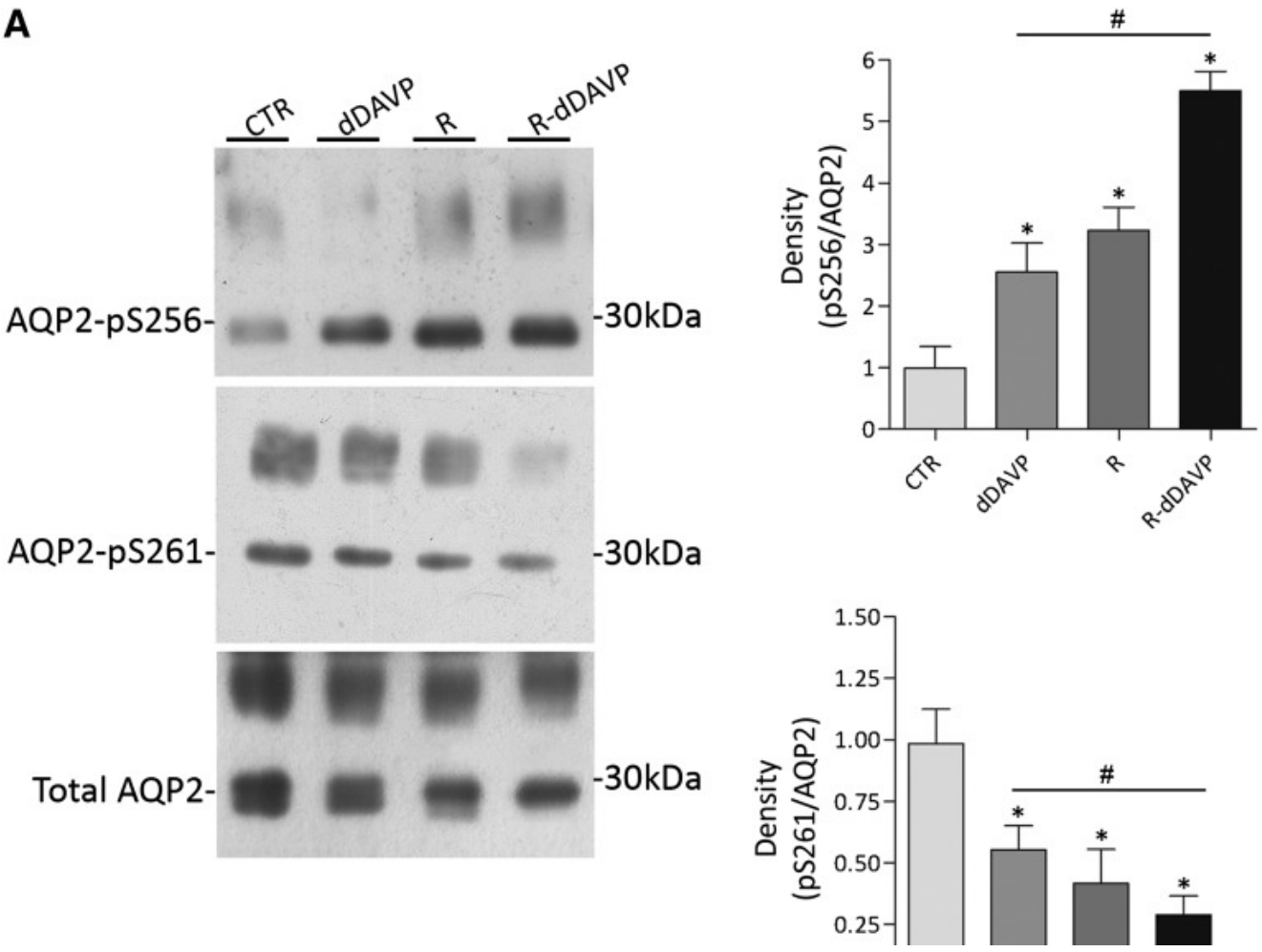

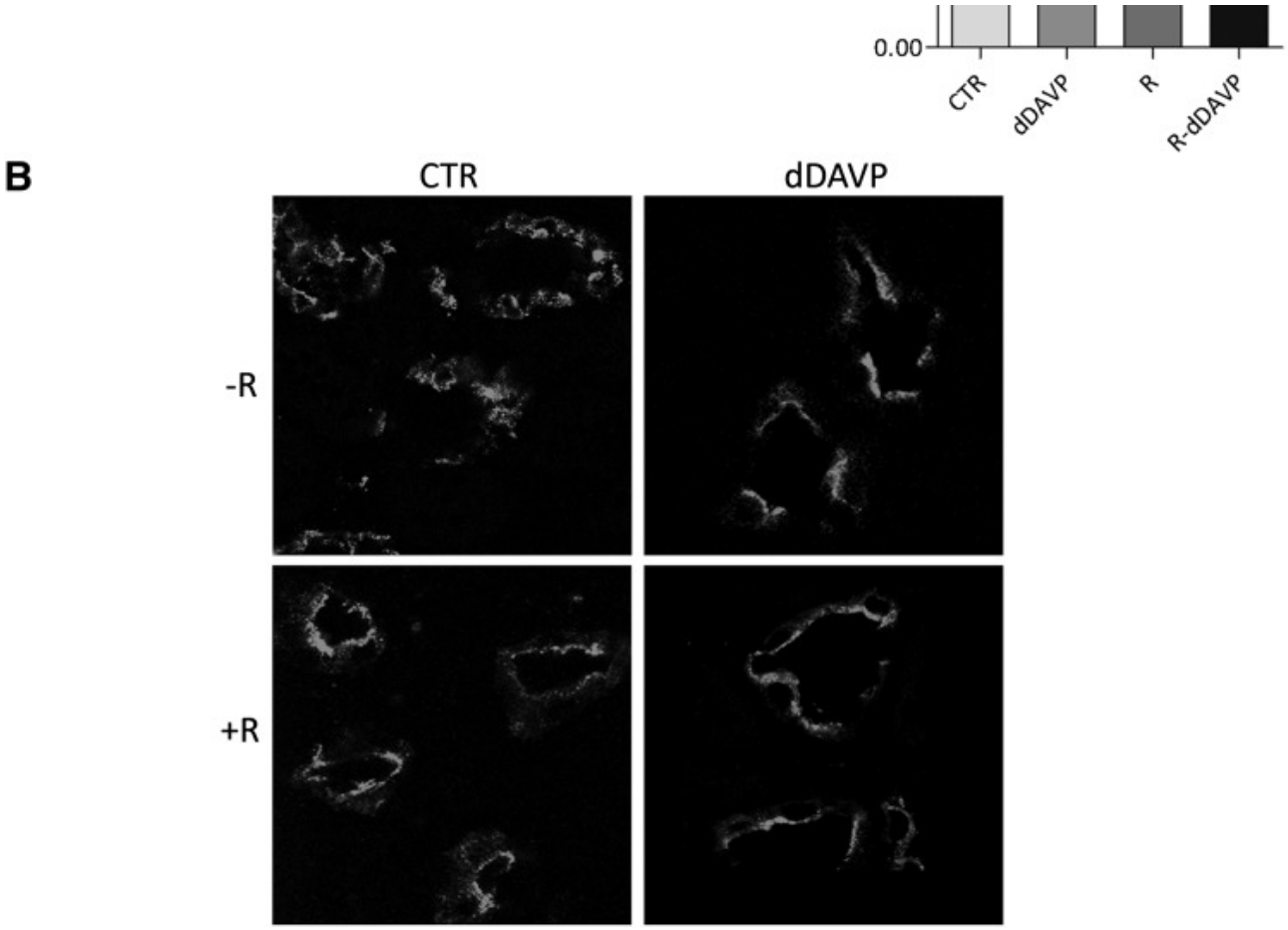

Effect of *R*-roscovitine on AQP2 phosphorylation and trafficking in rat kidney slices. (A) Effect of *R*-roscovitine on AQP2 S256 and S261 phosphorylations *ex vivo*. Rat kidney slices were treated as described in Concise Methods. Immunoprecipitated complexes were subjected to immunoblotting for total AQP2, AQP2-pS256, and AQP2-pS261. *R*-roscovitine increases AQP2-pS256, whereas it reduces AQP2-pS261. Signals were semiquantified by densitometry (right panel). *Samples significantly (means±SEMs; $P<0.05$) different from controls; $^{\#}$sample significantly (means±SEMs; $P<0.05$) different from dDAVP. (B) Effect of *R*-roscovitine on AQP2 distribution in renal kidney slices. Fresh renal slices were treated as described in Concise Methods, stained for AQP2, and subjected to confocal laser scanning microscopy (Leica TCS SP2 camera; Leica Microsystems). *R*-roscovitine (R) promotes AQP2 trafficking, regardless dDAVP stimulation.

Figure 3.

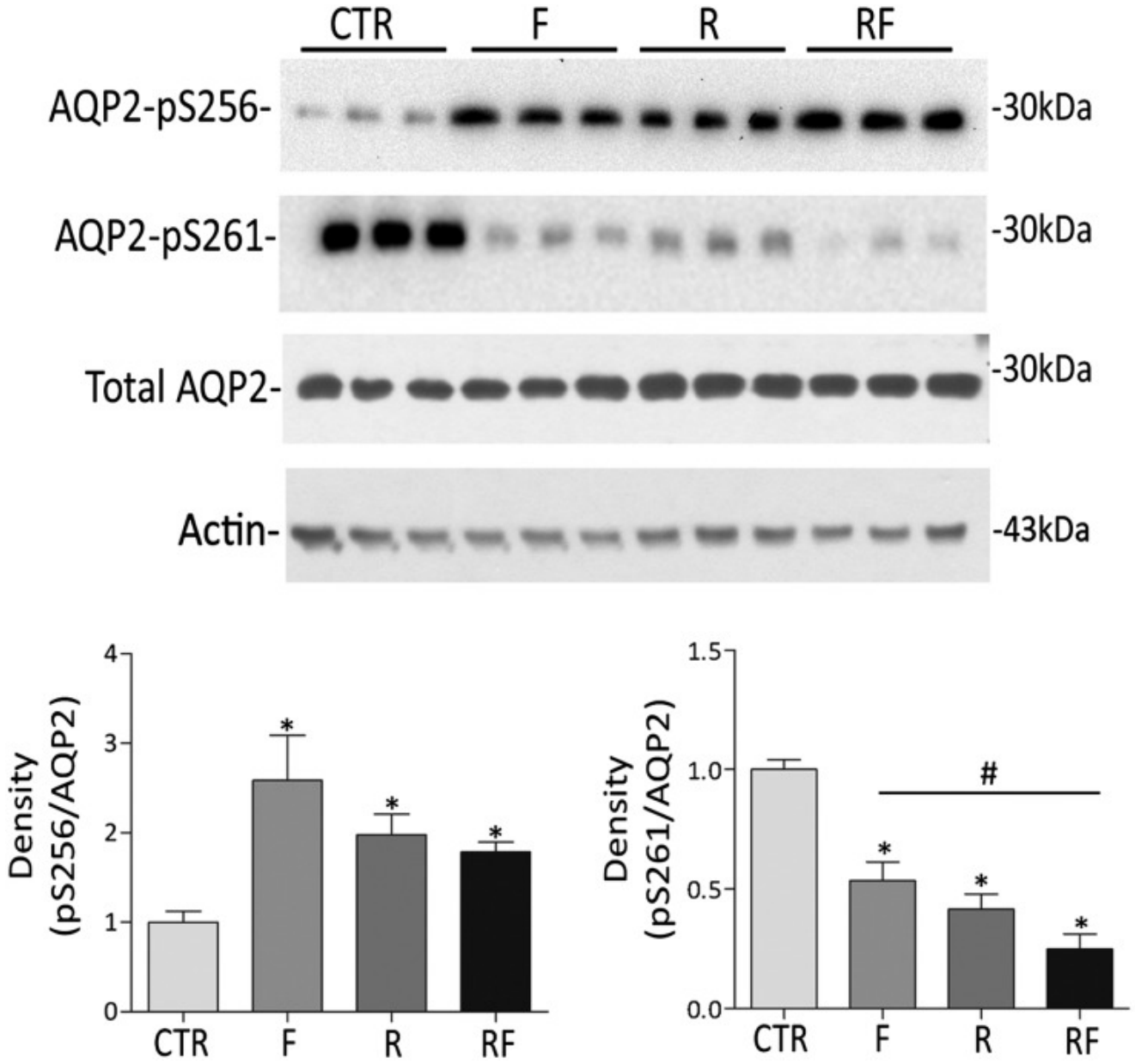

Effect of *R*-roscovitine on AQP2 S256 and S261 phosphorylation in MDCK-hAQP2 cells. MDCK-hAQP2 cells were left untreated (CTR) or stimulated with forskolin (F) in the absence (R) or the presence of *R*-roscovitine (RF). After treatments, cells were lysed and subjected to immunoprecipitation. Immunocomplexes were analyzed by immunoblotting for total AQP2, AQP2-pS256, and AQP2-pS261. *R*-roscovitine treatment increases AQP2-pS256, whereas reduces AQP2-pS261. Signals were semiquantified by densitometry (lower panel). *Samples significantly (means±SEMs; $P<0.05$) different from controls; $^{\#}$sample significantly (means±SEMs; $P<0.05$) different from forskolin condition. No change in the expression of the housekeeping protein actin was detected within the *R*-roscovitine incubation time used in this study.

Figure 4.

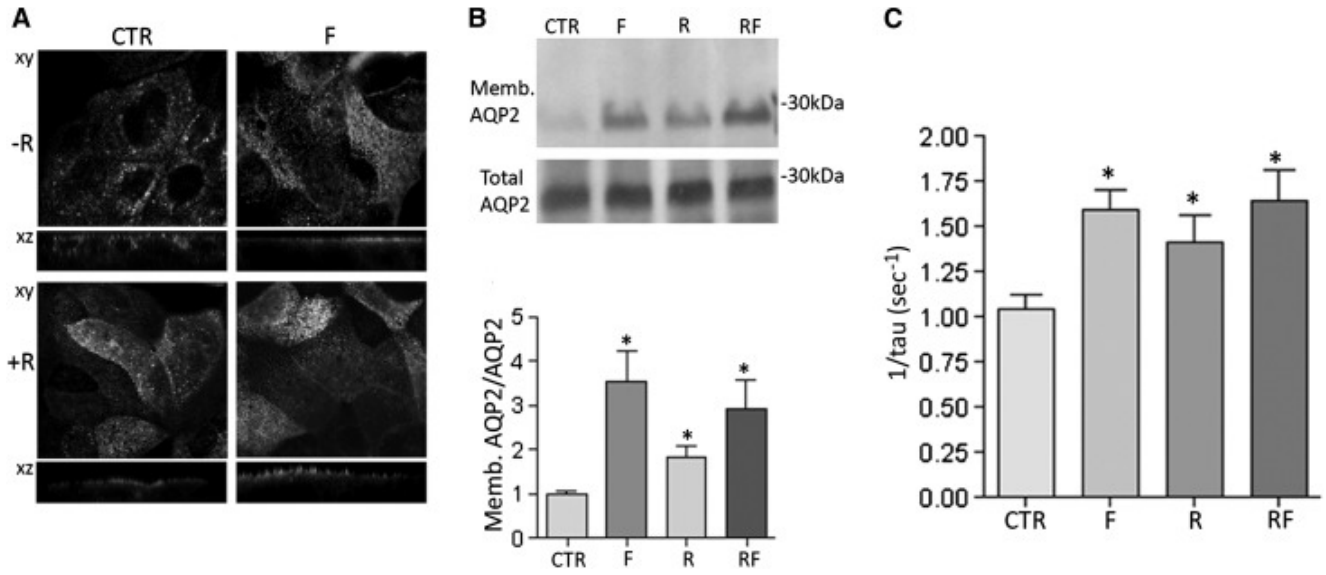

Effect of *R*-roscovitine on AQP2 trafficking and function. (A) MDCK-hAQP2 cells were treated as already described and subjected to immunofluorescence studies to visualize AQP2 specifically. Confocal analysis reveals that *R*-roscovitine (R) increases the cell surface expression of AQP2 compared with cells left under basal condition (CTR). (B) On treatments, cells were subjected to cell surface biotinylation assay with Biocityn Hydrazide. Immunoblotting analysis of total and apical AQP2 indicates that *R*-roscovitine incubation increases AQP2 abundance at the apical plasma membrane. Densitometric analysis of the 29-kD biotinylated AQP2 band (lower panel) normalized to total AQP2 (means±SEMs; **P* <0.05). (C) Time constant of cell swelling under hypotonic stimulus. Cells were grown and treated as described in Concise Methods. The time course of fluorescence changes in calcein-loaded cells indicates that *R*-roscovitine increases cell swelling ability regardless of forskolin stimulation (means±SEMs; **P*<0.05).

Figure 5.

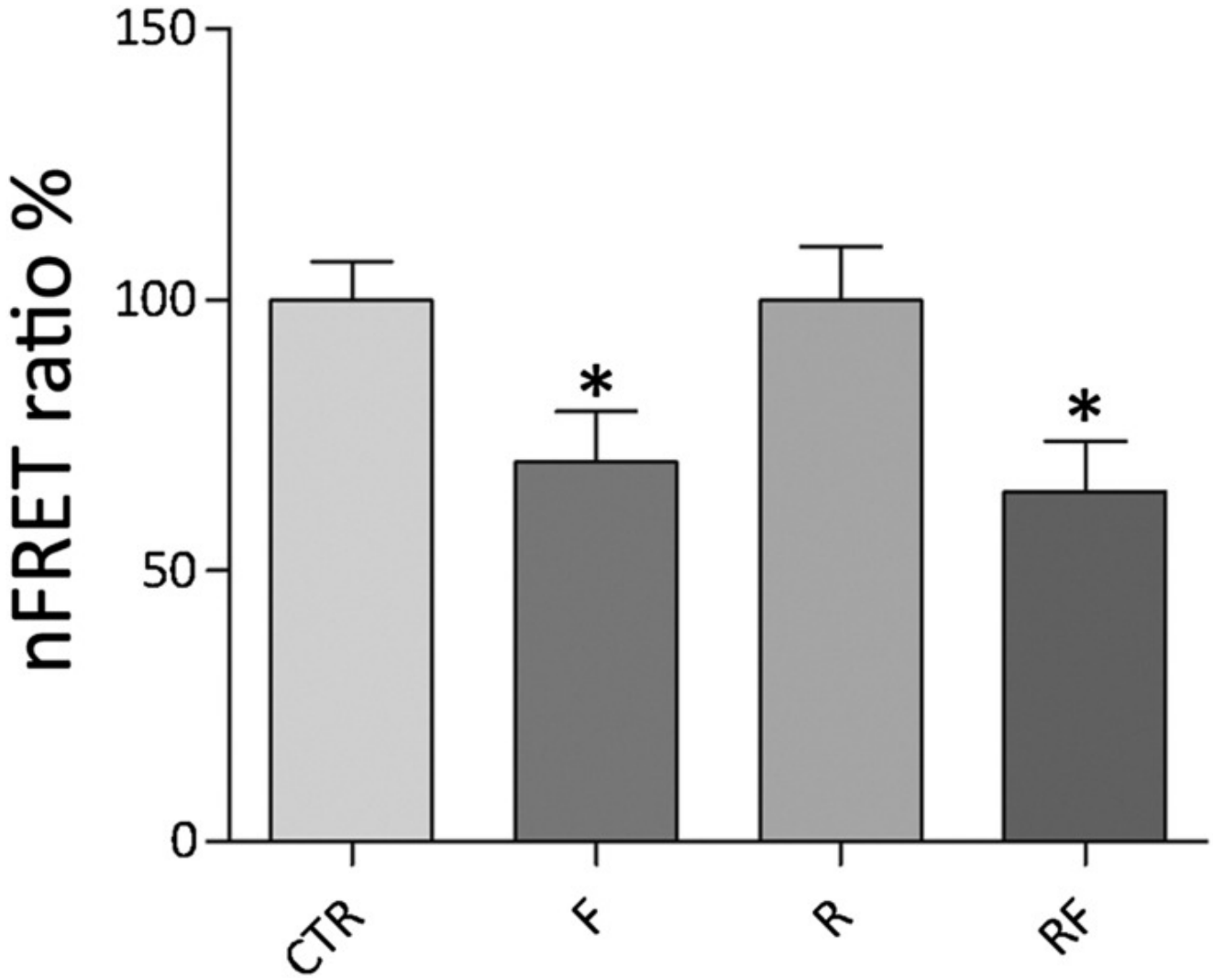

Evaluation of PKA activity by FRET analysis. Histogram (means±SEMs; *P<0.05) compares changes of normalized FRET ratio between forskolin (F), *R*-roscovitine (R), *R*-roscovitine in presence of forskolin (RF), and control conditions (CTR). FRET studies suggest that *R*-roscovitine does not affect PKA activity.

Figure 6.

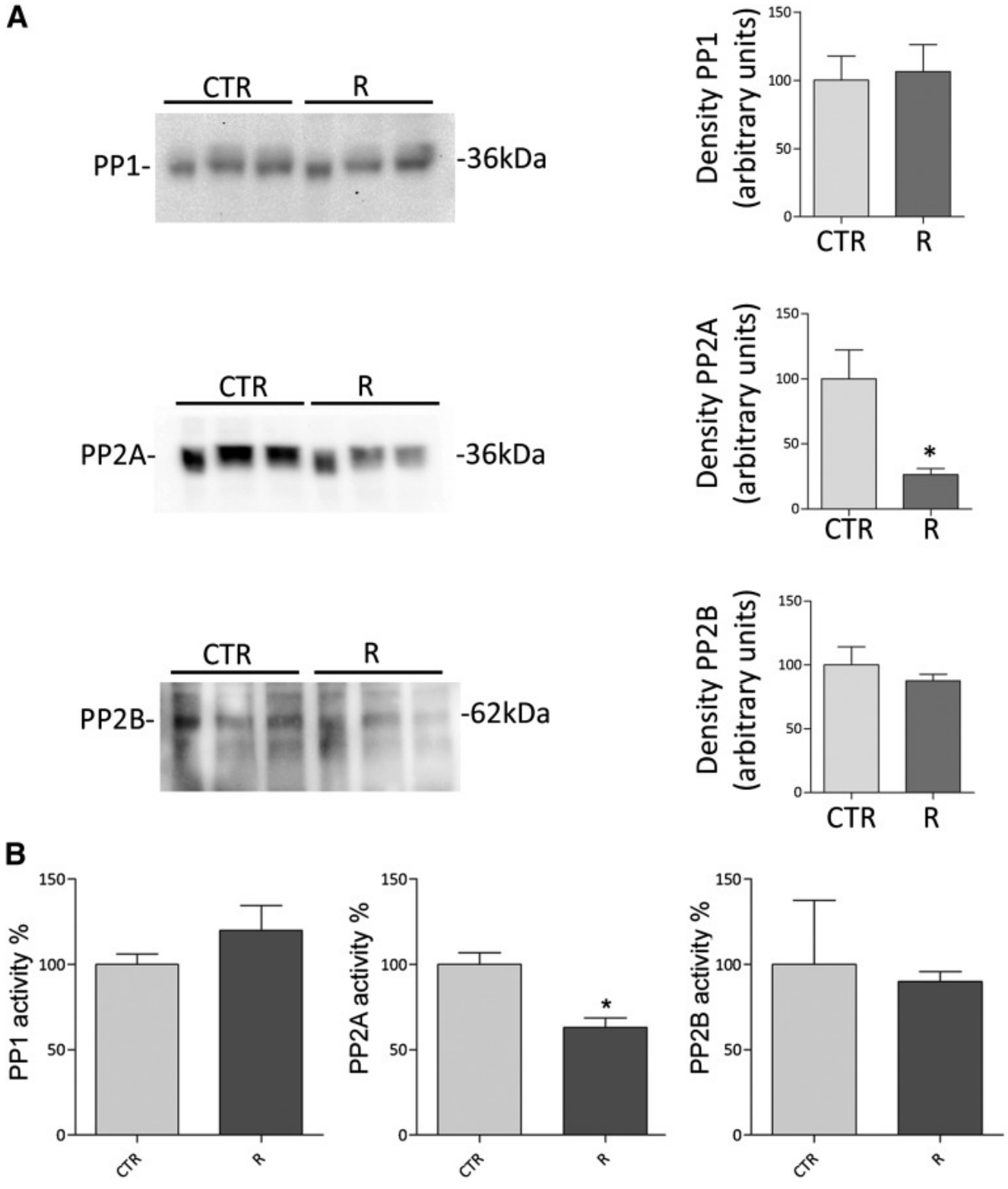

Effect of *R*-roscovitine on protein phosphatase expression and activity in MDCK-hAQP2 cells. (A) Immunoblotting expression studies of protein phosphatases PP1, PP2A, and PP2B in MDCK-hAQP2 cells. Equal amounts of proteins from MDCK-hAQP2 cells left untreated (CTR) or incubated with *R*-roscovitine (R) were subjected to electrophoresis and immunoblotted using specific antibodies as described in Concise Methods. Immunoreactive signals were semiquantified by densitometry (right panel), indicating that *R*-roscovitine reduces only PP2A protein content. (B) Protein phosphatase activities were evaluated using an immunoprecitation assay kit as described in Concise Methods. Data (means±SEMs;

*P<0.05) indicate that *R*-roscovitine decreases PP2A activity only.

Figure 7.

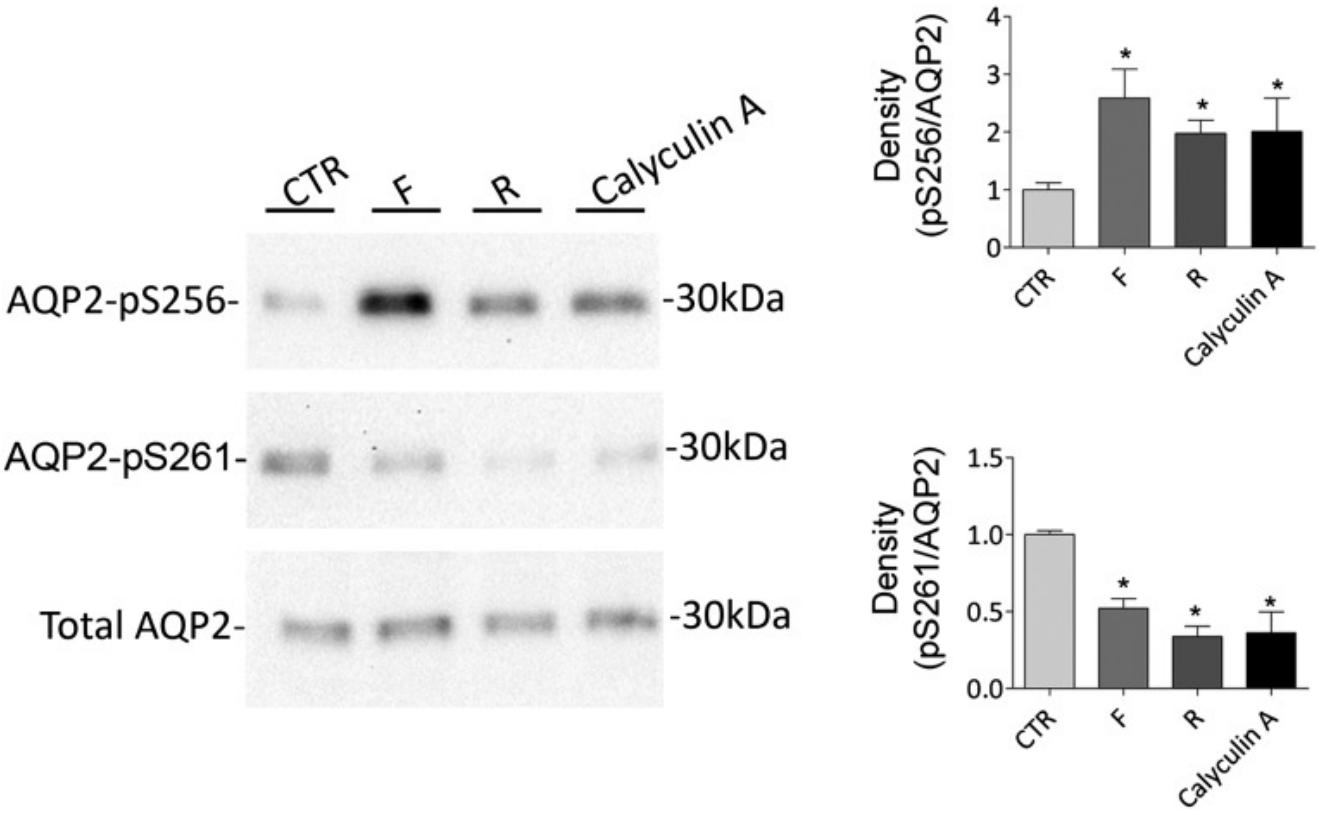

Effect of calyculin-A on AQP2 phosphorylation at S256 and S261. Cells were grown to confluence and left unstimulated (CTR) or treated with forskolin (F), *R*-roscovitine (R), or calyculin-A. Protein lysates were subjected to electrophoresis and immunoblotting using antibodies against AQP2 phosphorylated at S256, S261, or total AQP2 (indicated). Statistical analysis (right panel) revealed that calyculin-A, similarly to *R*-roscovitine, increased the abundance of AQP2-pS256, whereas it decreased AQP2-pS261 relative to unstimulated cells; S256 or S261 phosphorylation was normalized against total AQP2, and control conditions were set to one. *Significant difference (P<0.05).

Figure 8.

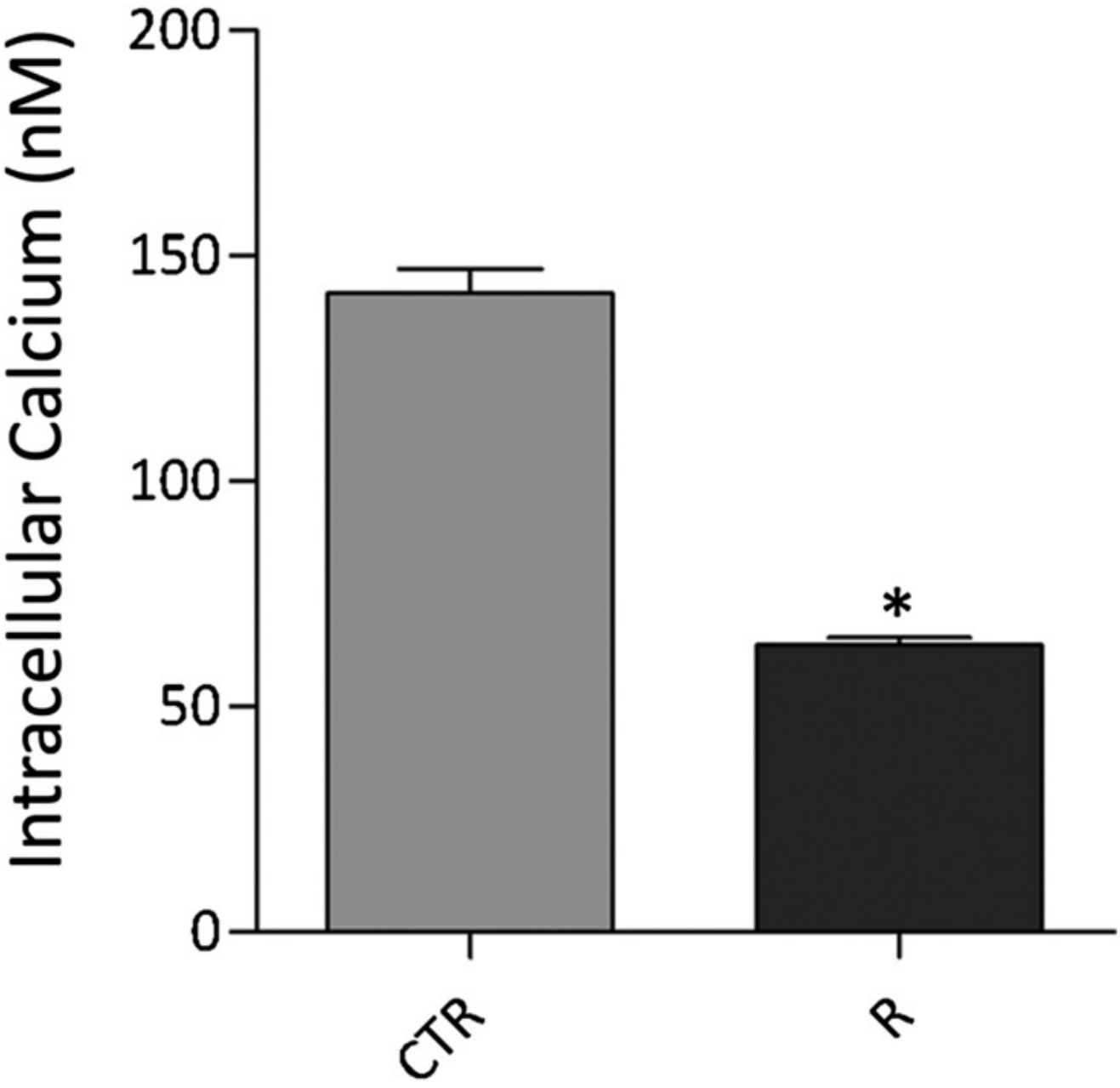

Effect of *R*-roscovitine on intracellular calcium content. MDCK cells were loaded with 4 μM Fura 2-AM for 15 minutes at 37°C in DMEM. Fluorescence measurements were carried out using Metafluor software (Molecular Devices, MDS Analytical Technologies). Free cytosolic [Ca^{2+}] was calculated accordingly to Grynkiewicz formula. Data (mean±SEMs; *P<0.001) revealed that *R*-roscovitine (R) reduced intracellular calcium concentration compared with cells left under basal condition (CTR).

Figure 9.

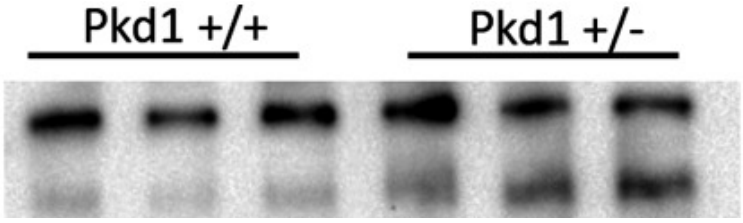

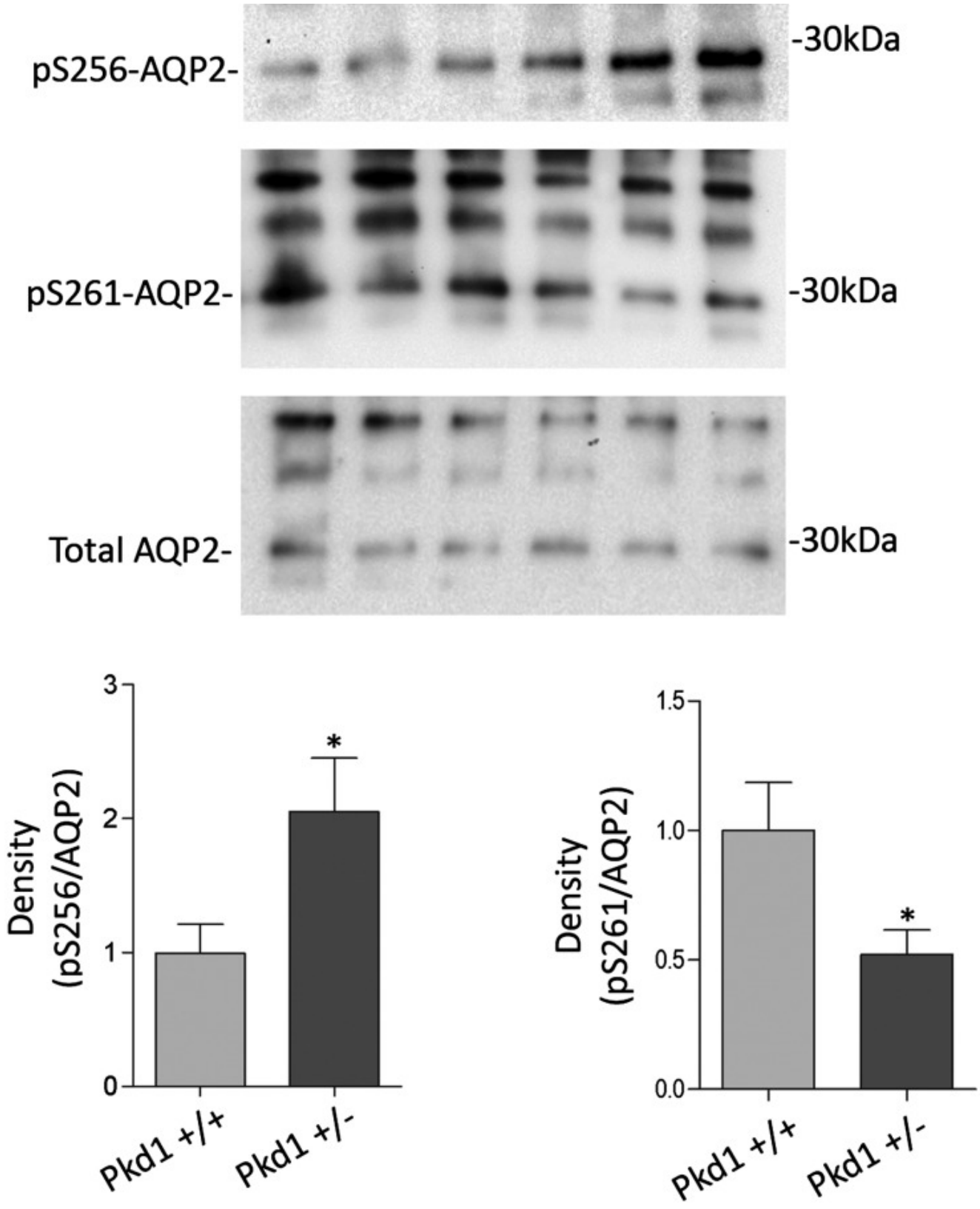

Phosphorylation of AQP2 at S256 and S261 in *Pkd1*$^{+/-}$ mice. Representative immunoblotting showing AQP2, AQP2-pS256, and AQP2-pS261 expression in kidneys isolated from *Pkd1*$^{+/-}$ mice compared with WT animals. Densitometry (on the right) indicates that AQP2-pS256 increases while pS261 decreases in *Pkd1*$^{+/-}$ mice. S256 and S261 phosphorylation was normalized against total AQP2, and control conditions were set to one. *Significant difference

($P<0.05$).

Figure 10.

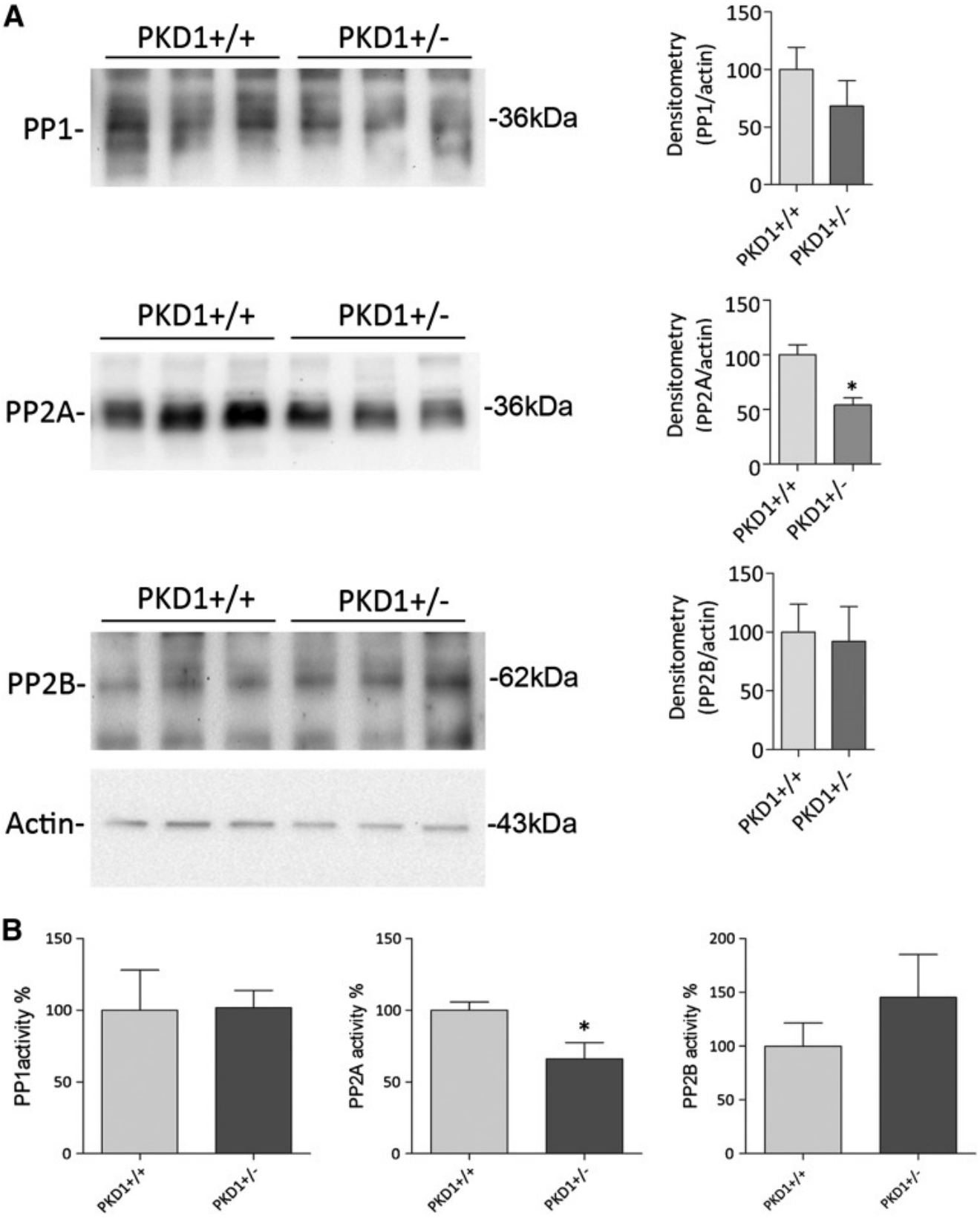

Protein phosphatase expression and activity in *Pkd1*$^{+/-}$ mice. (A) Immunoblotting evaluation of PP1, PP2A, and PP2B in *Pkd1*$^{+/-}$ mice. Equal amounts of proteins isolated from kidneys of WT and *Pkd1*$^{+/-}$ mice were subjected to electrophoresis and immunoblotted using specific antibodies, as described in Concise Methods. Immunoreactive signals were semiquantified by densitometry (right panel), indicating that only PP2A protein content decreases in *Pkd1*$^{+/-}$ mice significantly. (B) Protein phosphotase activities were evaluated using an immunoprecitation assay kit as described in Concise Methods. Data (means±SEMs; **P*<0.05) indicate that only PP2A activity is reduced in transgenic *Pkd1*$^{+/-}$ animals compared with WT mice.

Figure 11.

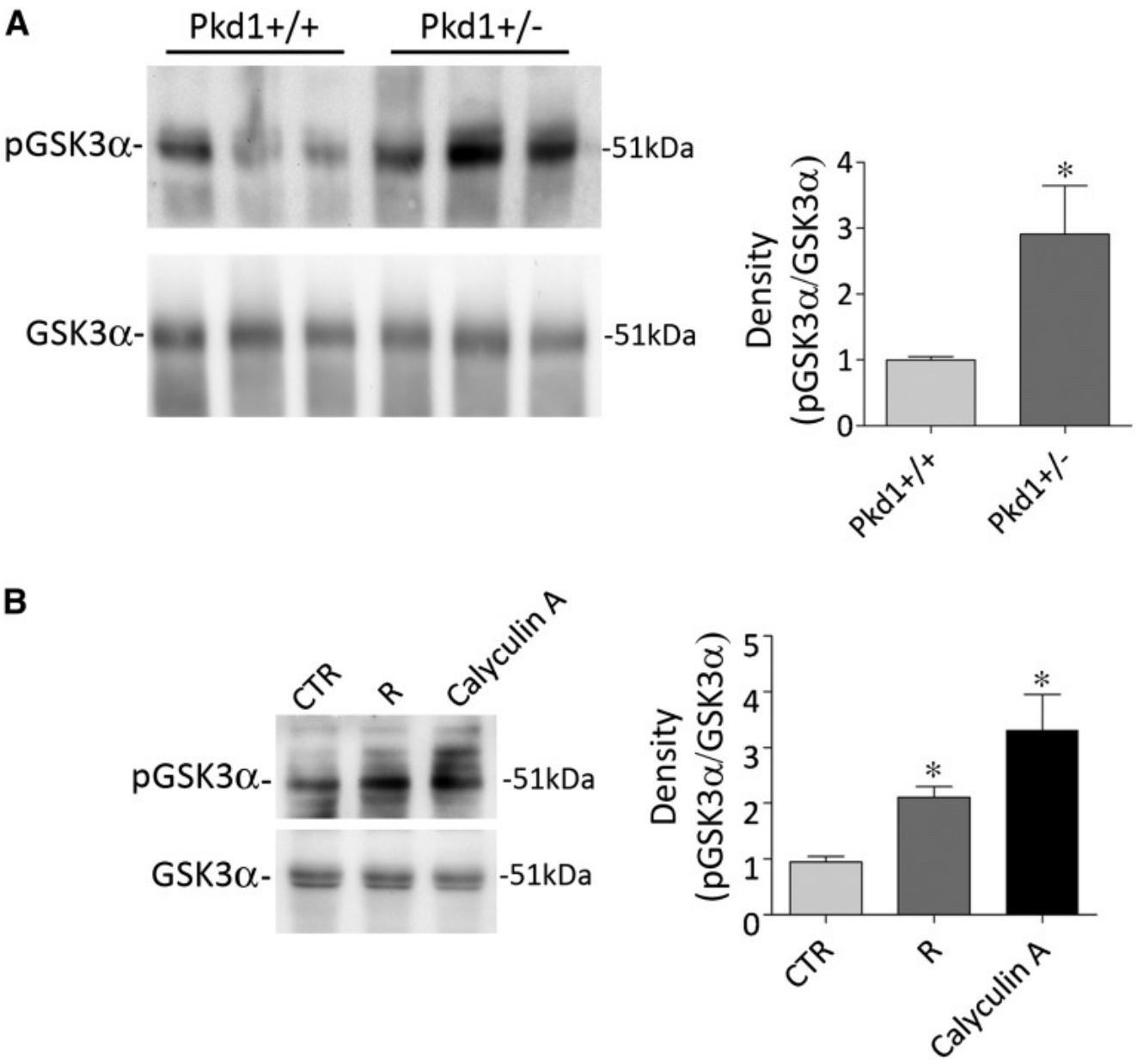

Phosphorylation of GSK3*α*. (A) Protein lysates isolated from *Pkd1*$^{+/-}$ mice and WT mice were subjected to electrophoresis and immunoblotting using antibodies against GSK3*α* and GSK3*α*-pS21. Statistical analysis (right panel) revealed that GSK3*α*-pS21 significantly increased in *Pkd1*$^{+/-}$ mice compared with the WT counterpart. GSK3*α* phosphorylation was normalized against total GSK3*α*, and GSK3*α*-pS21 in *Pkd1*$^{+/+}$ mice was set to one. *Significant

difference ($P<0.05$). (B) Rat renal kidney slices were prepared as described in Concise Methods. Total lysates from slices left untreated, stimulated with *R*-roscovitine, or stimulated with calyculin-A were subjected to immunoblotting for GSK3α and GSK3α-pS21. *R*-roscovitine and calyculin-A increase GSK3α-pS21. Signals were semiquantified by densitometry (right panel). Samples significantly (means±SEMs; *$P<0.05$) different from controls.

Figure 12.

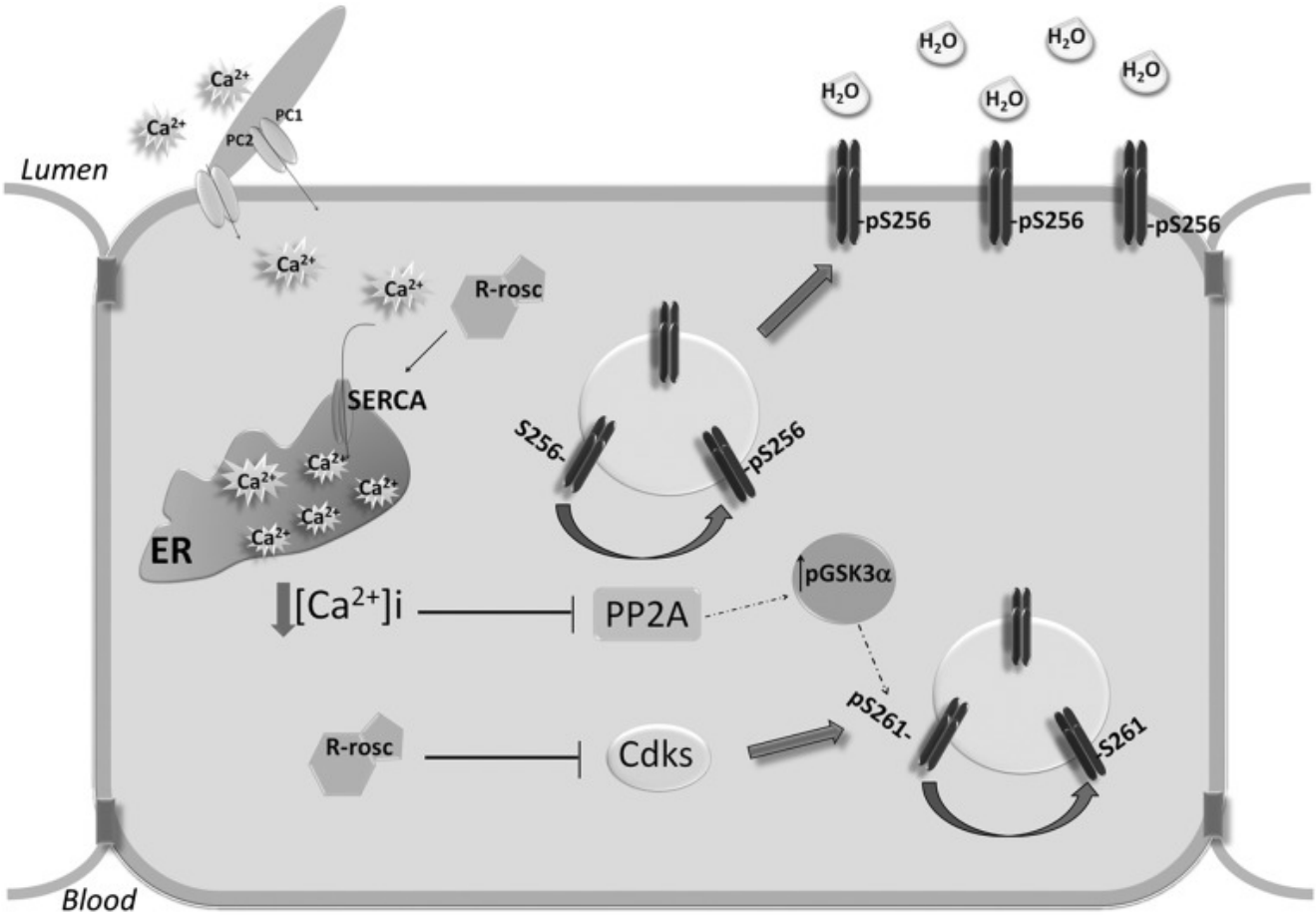

Identification of a PKA-independent pathway controlling AQP2 trafficking. Schematic model (detailed description in Discussion). ER, endoplasmic reticulum.

Articles from Journal of the American Society of Nephrology : JASN are provided here courtesy of **American Society of Nephrology**